Branching fractions and *CP* violation in $B^- \to K^+K^-\pi^-$ and $B^- \to \pi^+\pi^-\pi^-$ decays

Hai-Yang Cheng[1] and Chun-Khiang Chua[2]

[1]*Institute of Physics, Academia Sinica, Taipei, Taiwan 115, Republic of China*
[2]*Department of Physics and Center for High Energy Physics, Chung Yuan Christian University, Chung-Li,
Taiwan 320, Republic of China*

We present in this work a study of tree-dominated charmless three-body decays of *B* mesons, $B^- \to K^+K^-\pi^-$ and $B^- \to \pi^+\pi^-\pi^-$, within the factorization approach. The main results are: (i) There are two distinct sources of nonresonant contributions: one arises from the $b \to u$ tree transition and the other from the nonresonant matrix element of scalar densities $\langle M_1 M_2 | \bar{q}_1 q_2 | 0 \rangle^{\rm NR}$. It turns out that even for tree-dominated three-body decays, dominant nonresonant contributions originate from the penguin diagram rather than from the $b \to u$ tree process, as implied by the large nonresonant component observed recently in the $\pi^- K^+$ system which accounts for one third of the $B^- \to K^+K^-\pi^-$ rate. (ii) The calculated branching fraction of $B^- \to f_2(1270)\pi^- \to K^+K^-\pi^-$ is smaller than the LHCb by a factor of ~ 7 in its central value, but the predicted $\mathcal{B}(B^- \to f_2(1270)\pi^- \to \pi^+\pi^-\pi^-)$ is consistent with the data. Branching fractions of $B^- \to f_2(1270)\pi^-$ extracted from the LHCb measurements of these two processes also differ by a factor of seven! Therefore, it is likely that the $f_2(1270)$ contribution to $B^- \to K^+K^-\pi^-$ is largely overestimated experimentally. Including $1/m_b$ power corrections from penguin annihilation inferred from QCD factorization (QCDF), a sizable *CP* asymmetry of 25% in the $f_2(1270)$ component agrees with experiment. (iii) A fraction of 5% for the $\rho(1450)$ component in $B^- \to \pi^+\pi^-\pi^-$ is in accordance with the theoretical expectation. However, a large fraction of 30% in $B^- \to K^+K^-\pi^-$ is entirely unexpected. This issue needs to be clarified in the future. (iv) We study final-state $\pi\pi \leftrightarrow K\bar{K}$ rescattering and find that the rescattering contributions to both $B^- \to K^+K^-\pi^-$ and $B^- \to \pi^+\pi^-\pi^-$ seem to be overestimated experimentally by a factor 4. (v) Using the QCDF expression for the $B^- \to \sigma/f_0(500)\pi^-$ amplitude to study the decay $B^- \to \sigma\pi^- \to \pi^+\pi^-\pi^-$, the resultant branching fraction and *CP* violation of 15% agree with experiment. (vi) *CP* asymmetry for the dominant quasi-two-body decay mode $B^- \to \rho^0\pi^-$ was found by the LHCb to be consistent with zero in all three *S*-wave models. In the QCDF approach, $1/m_b$ power corrections, namely, penguin annihilation and hard spectator interactions contribute destructively to $\mathcal{A}_{CP}(B^- \to \rho^0\pi^-)$ to render it consistent with zero. (vii) A significant *CP* asymmetry has been seen in the $\rho^0(770)$ region for positive- and negative-helicity angle cosines. Considering the low $\pi^+\pi^-$ invariant mass region of the $B^+ \to \pi^+\pi^+\pi^-$ Dalitz plot of *CP* asymmetries divided into four zones, the pattern of *CP* violation in each zone is well described by the interference between $\rho(770)$ and $\sigma(500)$ as well as the nonresonant background.

I. INTRODUCTION

In 2013 and 2014 LHCb has measured direct *CP* violation in charmless three-body decays of *B* mesons [1–3] and found evidence of inclusive integrated *CP* asymmetries $\mathcal{A}_{CP}^{\rm incl}$ in $B^+ \to \pi^+\pi^+\pi^-$ (4.2σ), $B^+ \to K^+K^+K^-$ (4.3σ) and $B^+ \to K^+K^-\pi^+$ (5.6σ) and a 2.8σ signal of *CP* violation in $B^+ \to K^+\pi^+\pi^-$. The study of three-body decays allows to measure the distribution of *CP* asymmetry in the Dalitz plot. Hence, the Dalitz-plot analysis of $\mathcal{A}_{CP}$ distributions can reveal very rich information about *CP* violation. Besides the integrated *CP* asymmetry, local asymmetry varies in magnitude and sign from region to region. Indeed, LHCb has also observed large asymmetries in localized regions of phase space, such as the low invariant mass region and the rescattering regions of $m_{\pi^+\pi^-}$ or $m_{K^+K^-}$ between 1.0 and 1.5 GeV.

Recently LHCb has analyzed the decay amplitudes of $B^+ \to \pi^+\pi^-\pi^+$ and $B^+ \to K^+K^-\pi^+$ decays in the Dalitz plot [4–6]. Previously, the only amplitude analysis available at *B* factories was performed by *BABAR* for $B^+ \to \pi^+\pi^-\pi^+$ [7]. In the LHCb analysis of the
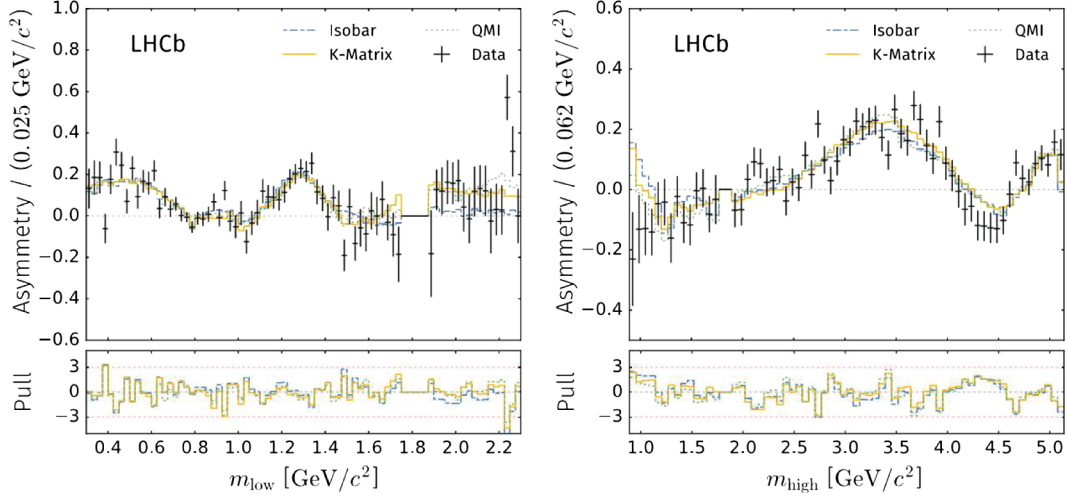
FIG. 1. CP asymmetries for $B^{\pm} \to \pi^{\pm}\pi^{+}\pi^{-}$ measured in the low invariant-masss $m(\pi^{+}\pi^{-})_{\text{low}}$ region (left panel) and high invariant-masss $m(\pi^{+}\pi^{-})_{\text{high}}$ region (right panel) in three different models for S-wave: the isobar model, the K-matrix model and the quasi-model-independent analysis. This plot is taken from [6].

$B^{\pm} \to \pi^{\pm}K^{+}K^{-}$ decay amplitudes, three contributions were considered in the $\pi^{\pm}K^{\mp}$ system, namely, $K^{*}(892)$ and $K_{0}^{*}(1430)$ resonances plus a nonresonant contribution, and four contributions in the $K^{+}K^{-}$ system: $\rho^{0}(1450)$, $f_{2}(1270)$, $\phi(1020)$ and an amplitude accounting for the $\pi\pi \leftrightarrow K\bar{K}$ rescattering [4]. The largest contribution with a fit fraction of 32% comes the nonresonant amplitude in the $\pi^{\pm}K^{\mp}$ system. A surprise comes from the quasi-two-body decay $B^{+} \to \rho(1450)\pi^{+}$ which accounts for 31% of the $K^{+}K^{-}\pi^{+}$ decays. This seems to imply an enormously large coupling of $\rho(1450)$ with $K^{+}K^{-}$. Another very interesting feature of this analysis is that almost all the observed CP asymmetry in this channel is observed in the rescattering amplitude, which is the largest CP violation effect observed from a single amplitude.

The LHCb analysis of the $B^{-} \to \pi^{+}\pi^{-}\pi^{-}$ decay amplitude [5,6] showed some highlights: (i) Instead of a large nonresonant S-wave contribution observed by *BABAR* [7], the isobar model S-wave amplitude was presented by the LHCb as the coherent sum of contributions from the σ [i.e., $f_{0}(500)$] meson and a $\pi\pi \leftrightarrow K\bar{K}$ rescattering amplitude within the mass range $1.0 < m_{\pi^{+}\pi^{-}} < 1.5$ GeV. A significant CP violation of 15% in $B^{+} \to \sigma\pi^{+}$ and a large CP asymmetry of order 45% in the rescattering amplitude were found by LHCb. (ii) CP asymmetries for $B^{\pm} \to \pi^{\pm}\pi^{+}\pi^{-}$ were measured in both low and high invariant-masss regions, see Fig. 1. The peak in the low-m_{low} region around 1.3 GeV is due to the resonance $f_{2}(1270)$. Indeed, the mode with $f_{2}(1270)$ exhibited a CP violation of 40%. It is very interesting to notice a large CP asymmetry also observed in the high-m_{high} region. (iii) CP violation in
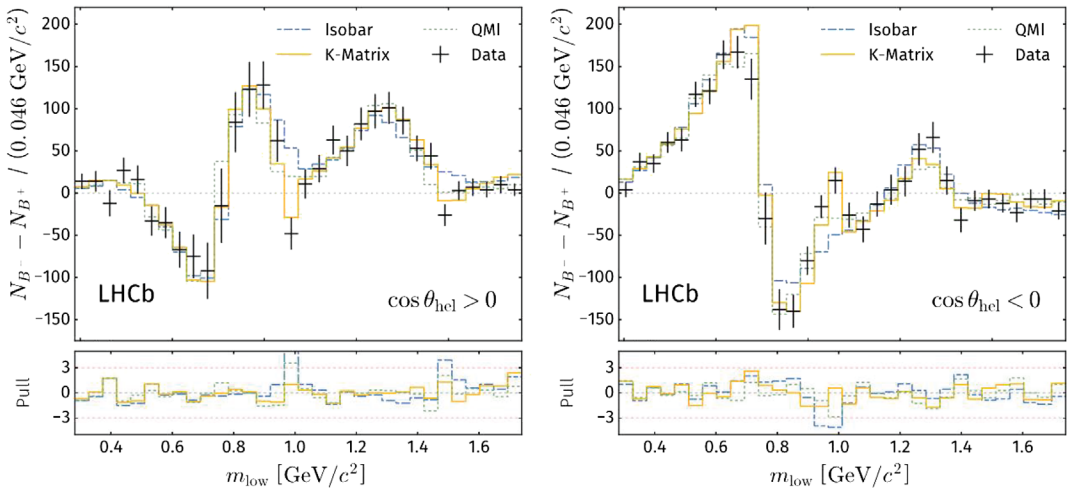

FIG. 2. The difference of $N_{B^{-}}$ and $N_{B^{+}}$, the number of B^{-} and B^{+} events respectively, for $B^{\pm} \to \pi^{\pm}\pi^{+}\pi^{-}$ measured in the low-m_{low} region for (a) $\cos\theta_{\text{hel}} > 0$ and (b) $\cos\theta_{\text{hel}} < 0$ with the helicity angle θ_{hel} being defined in Fig. 3. This plot is taken from [6].
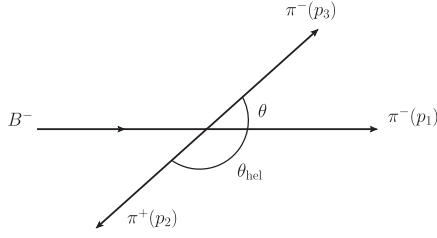
FIG. 3. The angle θ between the momenta of the two π^- pions measured in the rest frame of the dipion system in the decay $B^- \to \pi^-(p_1)\pi^+(p_2)\pi^-(p_3)$. It is related to the helicity angle θ_{hel} defined by the LHCb through the relation $\theta + \theta_{\text{hel}} = \pi$.

the quasi-two-body decay $B^+ \to \rho^0(770)\pi^+$ is measured to be consistent with zero in all three different S-wave approaches, contrary to the existing model calculations. Nevertheless, a significant *CP* asymmetry in the ρ^0 region can be seen in Fig. 2 where the data are separated by the sign of the value of $\cos\theta_{\text{hel}}$ with θ_{hel} being the helicity angle, evaluated in the $\pi^+\pi^-$ rest frame, between the pion with opposite charge to the B and the third pion from the B decay (see Fig. 3). This feature which was already noticed previously in [2] indicates that *CP* violation close to the $\rho(770)$ resonance is proportional to $(m_\rho^2 - m_{\text{low}}^2)\cos\theta_{\text{hel}}$. Hence, *CP* asymmetry in the $\rho(770)$ region arises from the interference between the $\rho(770)$ and S-wave contributions. The interference pattern observed in Fig. 2 will be destroyed by the *CP* violation in $B^+ \to \rho^0(770)\pi^+$ because it is proportional to $\cos^2\theta_{\text{hel}}$. This is again an indication of nearly vanishing $\mathcal{A}_{CP}(B^+ \to \rho^0\pi^+)$.

We have explored three-body B decays in [8–10] under the factorization approximation. In this work we shall update the analysis of three-body decays $B^+ \to \pi^+\pi^-\pi^+$ and $B^- \to K^+K^-\pi^+$ as the LHCb has presented the new amplitude analyses of them. Attention will be paid to integrated and regional *CP* violation. We take the factorization approximation as a working hypothesis rather than a first-principles starting point as factorization has not been proved for three-body B decays. Unlike the two-body case, to date we still do not have QCD-inspired theories for hadronic three-body decays, though attempts along the framework of pQCD and QCDF have been made in the past [11–13].

The layout of the present paper is as follows. In Sec. II we discuss the 3-body decay $B^- \to \pi^-K^+K^-$ and take into account the intermediate state contributions from $K^*(892)$

and $K_0^*(1430)$, $\rho^0(1450)$, $f_2(1270)$, and $\phi(1020)$, a non-resonant amplitude and an amplitude accounting for the $\pi\pi \leftrightarrow K\bar{K}$ rescattering. In Sec. III we focus on $B^- \to \pi^-\pi^+\pi^-$ decays. Since a clear *CP* violation is seen in three places as discussed before, we shall address these three sources of *CP* asymmetries. Attention is paid to the nearly vanishing *CP* violation in the quasi-two-body decay $B^- \to \rho^0\pi^-$ and *CP* violation induced by the interference between S- and P-wave amplitudes. Section IV comes to our conclusions. Input parameters for this work are summarized in the Appendix A. Appendix B is devoted to the flavor operators a_i^p used in this study. Since there are some confusions in the literature concerning the final-state rescattering formula, we shall go through the relevant derivations in Appendix C.

II. $B^\pm \to \pi^\pm K^+ K^-$ DECAYS

The charmless 3-body decays $B^- \to \pi^-K^+K^-$ has been studied at B factories by *BABAR* [14] and Belle [15] only for its branching fraction and direct *CP* asymmetry. On the theoretical side, this three-body decay mode was analyzed in [8–10] in which contributions from $K^*(892)$, $K_0^*(1430)$, $f_0(980)$ and a nonresonant amplitude were considered. The recent LHCb amplitude analysis takes into account a total of seven contributions: $K^*(892)$ and $K_0^*(1430)$, $\rho^0(1450)$, $f_2(1270)$, $\phi(1020)$, a nonresonant amplitude and an amplitude accounting for the $\pi\pi \leftrightarrow K\bar{K}$ rescattering. The results of the Dalitz plot analysis are shown in Table I [4]. The phases of $B^\pm$ decay amplitudes shown in the table include both weak and strong phases. Nonresonant contributions from both $\pi^\pm K^\mp$ and K^+K^- systems account for almost half of $B^\pm \to \pi^\pm K^+K^-$ rates. A very interesting feature is that the recattering amplitude, acting in the region $0.95 < m_{K^+K^-} < 1.42$ GeV, produced a large and negative *CP* asymmetry of $(-66 \pm 4 \pm 2)\%$, which is the largest *CP* violation effect observed from a single amplitude.

The explicit expression of the factorizable tree-dominated $B^- \to \pi^-(p_1)K^+(p_2)K^-(p_3)$ decay amplitude can be found in Eq. (5.1) of [9]. It can be decomposed as the coherent sum of resonant contributions together with the nonresonant background

$$A = \sum_R A_R + A_{\text{NR}}. \qquad (2.1)$$

TABLE I. Experimental results of the Dalitz plot fit for $B^\pm \to \pi^\pm K^+K^-$ decays taken from [4].

Contribution	Fit fraction (%)	$\mathcal{A}_{CP}(\%)$	B^+ phase (°)	B^- phase (°)
$K^*(890)^0$	$7.5 \pm 0.6 \pm 0.5$	$12.3 \pm 8.7 \pm 4.5$	0 (fixed)	0 (fixed)
$K_0^*(1430)^0$	$4.5 \pm 0.7 \pm 1.2$	$10.4 \pm 14.9 \pm 8.8$	$-176 \pm 10 \pm 16$	$136 \pm 11 \pm 21$
NR($\pi^\pm K^\mp$)	$32.3 \pm 1.5 \pm 4.1$	$-10.7 \pm 5.3 \pm 3.5$	$-138 \pm 7 \pm 5$	$166 \pm 6 \pm 5$
$\rho(1450)^0$	$30.7 \pm 1.2 \pm 0.9$	$-10.9 \pm 4.4 \pm 2.4$	$-175 \pm 10 \pm 15$	$140 \pm 13 \pm 20$
$f_2(1270)$	$7.5 \pm 0.8 \pm 0.7$	$26.7 \pm 10.2 \pm 4.8$	$-106 \pm 11 \pm 10$	$-128 \pm 11 \pm 14$
Rescattering	$16.4 \pm 0.8 \pm 1.0$	$-66.4 \pm 3.8 \pm 1.9$	$-56 \pm 12 \pm 18$	$-81 \pm 14 \pm 15$
$\phi(1020)$	$0.3 \pm 0.1 \pm 0.1$	$9.8 \pm 43.6 \pm 26.6$	$-52 \pm 23 \pm 32$	$107 \pm 33 \pm 41$

The resonant A_R and nonresonant $A_{\rm NR}$ amplitudes are referred to the decay processes with and without resonant contributions, respectively. Specifically, the resonant amplitude is related to the quasi-two-body decay process which is commonly described by the relativistic Breit-Wigner line shape model, while the rest (at the amplitude level) is ascribed to the nonresonant contribution. In general, the nonresonant signal originates from "direct" three-body B decays. Taking $B^- \to K^+ K^- \pi^-$ as an example, the nonresonant contributions in our framework based on factorization arise from the nonresonant components of the 3-body matrix element $\langle K^+ K^- | (V-A)_\mu | B^- \rangle$ and the 2-body matrix element of scalar density $\langle K^+ \pi^- | \bar{d}s | 0 \rangle$. Resonant contributions come from the resonant components of the above-mentioned 3-body and 2-body matrix elements. In addition, $\langle K^+ K^- | (V-A)_\mu | 0 \rangle$ is also governed by resonant contributions. The presence of the nonresonant $\langle K^+ \pi^- | \bar{d}s | 0 \rangle^{\rm NR}$ term induced by the penguin transition was first noticed by us together with A. Soni [8].

Experimentally, it is difficult to measure nonresonant contributions as the interference between the nonresonant and quasi-two-body amplitudes renders it difficult to disentangle these two distinct contributions and extract the nonresonant one. While both *BABAR* and Belle have adopted the parametrization

$$A_{\rm NR} = c_{12} e^{i\phi_{12}} e^{-\alpha s_{12}^2} + c_{13} e^{i\phi_{13}} e^{-\alpha s_{13}^2} + c_{23} e^{i\phi_{23}} e^{-\alpha s_{23}^2} \quad (2.2)$$

to describe the nonresonant three-body B decays, they differ in the analysis of nonresonant component in the $K\pi$ S-wave. By contrast, LHCb did not address this issue much. In the recent LHCb analysis of $B^\pm \to \pi^+ \pi^- \pi^\pm$ and $K^+ K^- \pi^\pm$ decays, only the nonresonant contribution in the $\pi^\pm K^\mp$ system has been studied by the LHCb in terms of a simple single-pole form factor of the type $(1 + m_{\pi^\pm K^\mp}^2 / \Lambda^2)^{-1}$ [4]. In the experimental analysis, it is also difficult to distinguish between the S-wave nonresonant background and the resonant state. For example, a large nonresonant $\pi^+ \pi^-$ S-wave contribution observed by *BABAR* in $B^+ \to \pi^+ \pi^- \pi^+$ decays [7] was presented by the LHCb as the coherent sum of contributions of the σ and a $\pi^+ \pi^- \leftrightarrow K^+ K^-$ rescattering amplitude.

A. Resonant contributions

In general, the intermediate vector, scalar and tensor resonances all can contribute to the three-body matrix element $\langle P_1 P_2 | J_\mu | B \rangle$, while only the scalar resonance contributes to $\langle P_1 P_2 | S | 0 \rangle$. Effects of intermediate resonances are described as a coherent sum of Breit-Wigner expressions. More precisely,[1]

$$\langle K^+(p_2) K^-(p_3) | (\bar{u}b)_{V-A} | B^- \rangle^R = \sum_i \frac{g^{V_i \to K^+ K^-}}{s_{23} - m_{V_i}^2 + i m_{V_i} \Gamma_{V_i}} \sum_{\rm pol} \varepsilon^* \cdot (p_2 - p_3) \langle V_i | (\bar{u}b)_{V-A} | B^- \rangle$$

$$+ \sum_i \frac{g^{f_{0i} \to K^+ K^-}}{s_{23} - m_{f_{0i}}^2 + i m_{f_{0i}} \Gamma_{f_{0i}}} \langle f_{0i} | (\bar{u}b)_{V-A} | B^- \rangle$$

$$+ \sum_i \frac{g^{f_{2i} \to K^+ K^-}}{s_{23} - m_{f_{2i}}^2 + i m_{f_{2i}} \Gamma_{f_{2i}}} \sum_{\rm pol} \varepsilon_{\mu\nu}^* p_2^\mu p_3^\nu \langle f_{2i} | (\bar{u}b)_{V-A} | B^- \rangle,$$

$$\langle K^+(p_2) K^-(p_3) | \bar{q} \gamma_\mu q | 0 \rangle^R = \sum_i \frac{g^{V_i \to K^+ K^-}}{s_{23} - m_{V_i}^2 + i m_{V_i} \Gamma_{V_i}} \sum_{\rm pol} \varepsilon^* \cdot (p_2 - p_3) \langle V_i | \bar{q} \gamma_\mu q | 0 \rangle,$$

$$\langle \pi^-(p_1) K^+(p_2) | (\bar{d}s)_{V-A} | 0 \rangle^R = \sum_i \frac{g^{K_i^{*0} \to K^+ \pi^-}}{s_{12} - m_{K_i^*}^2 + i m_{K_i^*} \Gamma_{K_i^*}} \sum_{\rm pol} \varepsilon^* \cdot (p_1 - p_2) \langle K_i^{*0} | (\bar{d}s)_{V-A} | 0 \rangle$$

$$+ \sum_i \frac{g^{K_{0i}^{*0} \to K^+ \pi^-}}{s_{12} - m_{K_{0i}^*}^2 + i m_{K_{0i}^*} \Gamma_{K_{0i}^*}} \langle K_{0i}^{*0} | (\bar{d}s)_{V-A} | 0 \rangle,$$

$$\langle K^+(p_2) K^-(p_3) | \bar{d}d | 0 \rangle^R = \sum_i \frac{g^{f_{0i} \to K^+ K^-}}{s_{23} - m_{f_{0i}}^2 + i m_{f_{0i}} \Gamma_{f_{0i}}} \langle f_{0i} | \bar{d}d | 0 \rangle,$$

$$\langle \pi^-(p_1) K^+(p_2) | \bar{d}s | 0 \rangle^R = \sum_i \frac{g^{K_{0i}^* \to K^+ \pi^-}}{s_{12} - m_{K_{0i}^*}^2 + i m_{K_{0i}^*} \Gamma_{K_{0i}^*}} \langle K_{0i}^{*0} | \bar{d}s | 0 \rangle, \quad (2.3)$$

---

[1]In [9,10] an additional minus sign was wrongly put in the Breit-Wigner propagator of the scalar resonance.

where $(\bar{q}_1 q_2)_{V-A} = \bar{q}_1 \gamma_\mu (1 - \gamma_5) q_2$. In practice, we shall only keep the leading resonances $V_i = \phi(1020), \rho(1450)$, $f_{0i} = f_0(980)$, $f_{2i} = f_2(1270)$, $K_i^* = K^*(892)$, and $K_{0i}^* = K_0^*(1430)$. We shall follow [16] for the definition of $B \to P$ and $B \to V$ transition form factors, [17] for form

factors in $B \to S$ transitions and [18] for $B \to T$ transition form factors.[2]

In the following we show the amplitudes from various resonances:

(1) K^*, K_0^*:

$$A_{K^*,K_0^*} = \left\{ F_1^{BK}(s_{12}) F_1^{K\pi}(s_{12}) \left[s_{23} - s_{13} - \frac{(m_B^2 - m_K^2)(m_K^2 - m_\pi^2)}{s_{12}} \right] \right.$$
$$\left. + F_0^{BK}(s_{12}) F_0^{K\pi}(s_{12}) \frac{(m_B^2 - m_K^2)(m_K^2 - m_\pi^2)}{s_{12}} \right\} \left(a_4^p - \frac{1}{2} a_{10}^p \right)$$
$$+ \frac{m_B^2 - m_K^2}{m_b - m_s} F_0^{BK}(s_{12}) m_{K_0^*} \bar{f}_{K_0^*} R_{K_0^*}(s_{12})(-2a_6^p + a_8^p), \tag{2.4}$$

where

$$R_{K_0^*}(s) = \frac{1}{s - m_{K_0^*}^2 + im_{K_0^*}\Gamma_{K_0^*}},$$

$$F_1^{K\pi}(s) = \frac{f_{K^*} m_{K^*} g^{K^* \to K^+ \pi^-}}{s - m_{K^*}^2 + im_{K^*}\Gamma_{K^*}},$$

$$F_0^{K\pi}(s) = F_1^{K\pi}(s) - f_{K_0^*} g^{K_0^* \to K^+ \pi^-} R_{K_0^*}(s) \frac{s}{m_K^2 - m_\pi^2}. \tag{2.5}$$

Notice two different types of the decay constant for K_0^*: $f_{K_0^*}$ and $\bar{f}_{K_0^*}$. They are defined by $\langle K_0^*(p)|(\bar{d}s)_{V-A}|0\rangle = if_{K_0^*} p_\mu$ and $\langle K_0^*|\bar{d}s|0\rangle = m_{K_0^*} \bar{f}_{K_0^*}$, respectively.

(2) $f_0(980)$

It has the similar expression as the amplitude of $B^- \to \sigma/f_0(500)\pi^- \to \pi^+ \pi^- \pi^-$ as will be discussed in detail in the next section. Here we write down the amplitude

$$A_{f_0(980)} = \frac{g^{f_0 \to K^+ K^-}}{s_{23} - m_{f_0}^2 + im_{f_0}\Gamma_{f_0}} \left\{ X^{(Bf_0,\pi)}(m_\pi^2)[a_1\delta_{pu} + a_4^p + a_{10}^p - (a_6^p + a_8^p)r_\chi^\pi]_{f_0\pi} \right.$$
$$\left. + \bar{X}^{(B\pi,f_0)} \left[a_2\delta_{pu} + 2(a_3^p + a_5^p) + \frac{1}{2}(a_7^p + a_9^p) + a_4^p - \frac{1}{2}a_{10}^p - \left(a_6^p - \frac{1}{2}a_8^p \right) \bar{r}_\chi^{f_0} \right]_{\pi f_0} \right\}, \tag{2.6}$$

where

$$X^{(Bf_0,\pi)} = -f_\pi(m_B^2 - s_{23}) F_0^{Bf_0^u}(m_\pi^2),$$
$$\bar{X}^{(B\pi,f_0)} = \bar{f}_{f_0}^d (m_B^2 - m_\pi^2) F_0^{B\pi}(s_{23}), \tag{2.7}$$

and

$$r_\chi^\pi(\mu) = \frac{2m_\pi^2}{m_b(\mu)(m_u + m_d)(\mu)},$$

$$\bar{r}_\chi^{f_0}(\mu) = \frac{2m_{f_0}}{m_b(\mu)}. \tag{2.8}$$

The order of the arguments of the $a_i^p(M_1 M_2)$ coefficients is dictated by the subscript $M_1 M_2$ given in Eq. (2.6). The superscript u of the form factor $F_0^{Bf_0^u}$ reminds us that it is the $u\bar{u}$ quark content that gets involved in the B to f_0 form factor transition. Likewise, the superscript d of the scalar decay constant $\bar{f}_{f_0}^d$ refers to the d quark component of the $f_0(980)$.

(3) $\phi(1020)$

$$A_{\phi(1020)} = -\frac{m_\phi f_\phi g^{\phi \to K^+ K^-}}{s_{23} - m_\phi^2 + im_\phi\Gamma_\phi}(s_{12} - s_{13}) F_1^{B\pi}(s_{23})$$
$$\times \left[a_3 + a_5 - \frac{1}{2}(a_7 + a_9) \right]. \tag{2.9}$$

Since contributions from the matrix elements $\langle\phi|(\bar{u}b)_{V-A}|B^-\rangle$ and $\langle K^+ K^-|(\bar{q}q)_{V-A}|0\rangle$ with $q = u$, d to the ϕ production are very suppressed, their effects will not be taken into account.

---

[2]The $B \to T$ transition form factors defined in [18,19] are different by a factor of i. We shall use the former as they are consistent with the normalization of $B \to S$ transition given in [17].

(4) $\rho(1450)$

$$A_{\rho(1450)} = -\frac{1}{\sqrt{2}} \frac{g^{\rho' \to K^+ K^-}}{s_{23} - m_{\rho'}^2 + im_{\rho'}\Gamma_{\rho'}} (s_{12} - s_{13}) \left\{ \frac{f_\pi}{2} \left[2m_{\rho'} A_0^{B\rho'}(m_\pi^2) \right. \right.$$
$$+ \left(m_B - m_{\rho'} - \frac{m_B^2 - s_{23}}{m_B + m_{\rho'}} \right) A_2^{B\rho'}(m_\pi^2) \right] [a_1 \delta_{pu} + a_4^p + a_{10}^p - (a_6^p + a_8^p) r_\chi^\pi]$$
$$+ m_{\rho'} f_{\rho'} F_1^{B\pi}(s_{23}) \left[a_2 \delta_{pu} - a_4^p + \frac{3}{2}(a_7 + a_9) + \frac{1}{2} a_{10}^p \right] \right\}, \tag{2.10}$$

with $\rho' = \rho(1450)$, where use of the relation

$$2m_V A_3^{BV}(q^2) = (m_B + m_V) A_1^{BV}(q^2) - (m_B - m_V) A_2^{BV}(q^2) \tag{2.11}$$

has been made.

(5) $f_2(1270)$

$$A_{f_2(1270)} = \frac{1}{\sqrt{2}} \frac{2m_{f_2}}{m_B} \frac{f_\pi g^{f_2 \to K^+ K^-}}{s_{23} - m_{f_2}^2 + im_{f_2}\Gamma_{f_2}}$$
$$\times \epsilon^{*\mu\nu}(\lambda) p_{2\mu} p_{3\nu} \epsilon_{\alpha\beta}(\lambda) p_B^\alpha p_1^\beta A_0^{Bf_2}(m_\pi^2)$$
$$\times [a_1 \delta_{pu} + a_4^p + a_{10}^p - (a_6^p + a_8^p) r_\chi^\pi]. \tag{2.12}$$

In the approach of QCD factorization (QCDF) [20], the decay amplitude of $B^- \to f_2(1270)\pi^-$ receives an additional contribution proportional to (see Eq. (B.8) of [19])

$$f_{f_2} F_1^{B\pi}(m_{f_2}^2) \left[a_2 \delta_{pu} + 2(a_3^p + a_5^p) + a_4^p \right.$$
$$\left. + r_\chi^{f_2} a_6^p + \frac{1}{2}(a_7^p + a_9^p) - \frac{1}{2}(a_{10}^p + r_\chi^{f_2} a_8^p) \right]. \tag{2.13}$$

The reader is referred to [19] for the definition of the decay constant f_{f_2} and the chiral factor $r_\chi^{f_2}$. As stressed in [19], the factorizable amplitude $\langle f_2 | J^\mu | 0 \rangle \langle \pi^- | J'_\mu | B^- \rangle$ vanishes in the factorization approach as the tensor meson cannot be produced through the $V - A$ or tensor current. Nevertheless, beyond the factorization approximation, contributions proportional to the decay constant f_{f_2} can be produced from vertex, penguin and spectator-scattering corrections.

Using the relation

$$\sum_\lambda \epsilon_{\mu\nu}(\lambda) \epsilon_{\rho\sigma}^*(\lambda) = \frac{1}{2} M_{\mu\rho} M_{\nu\sigma} + \frac{1}{2} M_{\mu\sigma} M_{\nu\rho} - \frac{1}{3} M_{\mu\nu} M_{\rho\sigma}, \tag{2.14}$$

with $M^{\mu\nu} = g^{\mu\nu} - P^\mu P^\nu / m_{f_2}^2$ and $P = p_2 + p_3$, it is straightforward to show that [21]

$$\sum_\lambda \epsilon^{*\mu\nu}(\lambda) \epsilon_{\alpha\beta}(\lambda) p_{2\mu} p_{3\nu} p_B^\alpha p_1^\beta = \frac{1}{3}(|\vec{p}_1||\vec{p}_2|)^2 - (\vec{p}_1 \cdot \vec{p}_2)^2, \tag{2.15}$$

with

$$|\vec{p}_1| = \left(\frac{(m_B^2 - m_\pi^2 - s_{23})^2}{4s_{23}} - m_\pi^2 \right)^{1/2},$$
$$|\vec{p}_2| = |\vec{p}_3| = \frac{1}{2}\sqrt{s_{23} - 4m_K^2}, \tag{2.16}$$

and

$$\vec{p}_1 \cdot \vec{p}_2 = \frac{1}{4}(s_{13} - s_{12}), \tag{2.17}$$

where $\vec{p}_1$ and $\vec{p}_2$ are the momenta of the $\pi^-(p_1)$ and $K^+(p_2)$ measured in the rest frame of the dikaon $K^+(p_2)$ and $K^-(p_3)$. However, the predicted CP asymmetry is of order -0.01 which is wrong in sign and magnitude compared to experiment, especially a large CP violation of 40% observed in the decay $B^- \to \pi^- f_2(1270) \to \pi^- \pi^+ \pi^-$. We thus follow the QCDF calculation in [19] to include $1/m_b$ power corrections arising from penguin annihilation (see Eq. (B.8) in [19]). This amounts to adding the penguin annihilation contributions $\beta_2^p \delta_{pu} + \beta_3^p + \beta_{3,\text{EW}}^p$ to the […] term in Eq. (2.12). Therefore, the amplitude $A_{f_2(1270)}$ reads

$$A_{f_2(1270)} = \sqrt{2} \frac{m_{f_2}}{m_B} \frac{f_\pi g^{f_2 \to K^+ K^-}}{s_{23} - m_{f_2}^2 + im_{f_2}\Gamma_{f_2}}$$
$$\times A_0^{Bf_2}(m_\pi^2) \left[\frac{1}{3}(|\vec{p}_1||\vec{p}_2|)^2 - (\vec{p}_1 \cdot \vec{p}_2)^2 \right]$$
$$\times [a_1 \delta_{pu} + a_4^p + a_{10}^p - (a_6^p + a_8^p) r_\chi^\pi$$
$$+ \beta_2^p \delta_{pu} + \beta_3^p + \beta_{3,\text{EW}}^p]. \tag{2.18}$$

Numerically, we shall follow [19] to use

$$\beta_2^p(f_2\pi) = 0.023 - i0.011,$$
$$(\beta_3^p + \beta_{3,\text{EW}}^p)(f_2\pi) = -0.047 + i0.053. \tag{2.19}$$

It should be remarked that the angular momentum distribution for the vector or tensor intermediate state is

not put by hand. It will come out automatically in the factorization approach. For example, the decay amplitude of $\rho(1450)$ or ϕ production contains a term $(s_{12} - s_{13})$ which is proportional to $\vec{p}_1 \cdot \vec{p}_2 = |p_1||p_2|\cos\theta_{12}$ [see Eq. (2.17)]. Likewise, the angular distribution of a tensor meson decaying into two spin-zero particles is governed by $(3\cos^2\theta_{12} - 1)$ [cf. Eq. (2.15)]. In general, the angular momentum distribution is described by the Legendre polynomial $P_J(\cos\theta)$.

B. Nonresonant contributions

The nonresonant contributions arise from the 3-body matrix element $\langle K^+(p_2)K^-(p_3)|(\bar{u}b)_{V-A}|B^-\rangle^{\mathrm{NR}}$ in the K^+K^- system and the 2-body matrix element of scalar density $\langle \pi^-(p_1)K^+(p_2)|\bar{d}s|0\rangle^{\mathrm{NR}}$ in the π^-K^+ system. The nonresonant contribution to the three-body matrix element can be parametrized in terms of four unknown form factors. The general expression of the nonresonant amplitude in the K^+K^- system induced from the $b \to u$ tree transition reads

$$A_{\mathrm{NR}}^{\mathrm{HMChPT}}$$
$$\equiv \langle K^+(p_2)K^-(p_3)|(\bar{u}b)_{V-A}|B^-\rangle^{\mathrm{NR}}\langle\pi^-(p_1)|(\bar{d}u)_{V-A}|0\rangle$$
$$= -\frac{f_\pi}{2}[2m_\pi^2 r + (m_B^2 - s_{23} - m_\pi^2)\omega_+ + (s_{12} - s_{13})\omega_-],$$
$$(2.20)$$

where the form factors r and $\omega_\pm$ can be calculated using heavy meson chiral perturbation theory (HMChPT) [22,23]. However, HMChPT is applicable only when the two scalars K^+ and K^- in $B \to K^+K^-$ transition are soft. Indeed, the predicted nonresonant rate, of order 33×10^{-6} in branching fraction, based on HMChPT will be one order of magnitude larger than the world average of the total branching fraction $\sim 5.2 \times 10^{-6}$. Hence, we shall assume the momentum dependence of nonresonant amplitudes in an exponential form [8]

$$A_{\mathrm{NR}}^{K^+K^-} = A_{\mathrm{NR}}^{\mathrm{HMChPT}}e^{-\alpha_{\mathrm{NR}}p_B\cdot(p_2+p_3)}$$
$$\times [a_1\delta_{pu} + a_4^p + a_{10}^p - (a_6^p + a_8^p)r_\chi^\pi], \quad (2.21)$$

in analog to Eq. (2.2), so that the HMChPT results are recovered in the soft meson limit $p_2, p_3 \to 0$. For the parameter α_{NR} we shall use $\alpha_{\mathrm{NR}} = 0.160$ GeV^{-2}.[3]

The extrapolation from the soft meson limit where HMChPT is applicable to the physical kinematic region through Eq. (2.21) is our main ansatz for the tree

nonresonant amplitude. In the literature, similar $B \to \pi\pi$ form factors in $B \to \pi\pi\pi$ decays have been studied extensively [24–30]. In the kinematic regime where the dipion state has a large energy and a low invariant mass, $\bar{B}^0 \to \pi^+\pi^0$ form factors have been studied using QCD light-cone sum rules with B-meson distribution amplitudes [28–30]. The interference of $\rho(770)$ with the excited ρ resonances such as $\rho(1450)$ and $\rho(1750)$ are regarded as effective "nonresonant" contributions. At low recoil (low q^2) and small dipion invariant mass, form factors for the pion-pion system have been treated in dispersion theory [25]. One can match dispersion theory with HMChPT to fix the subtraction constant and access the low-energy-region physics. In this work we will not use the results from light-cone sum rules or dispersion theory as the nonresonant contributions there are not specified separately and explicitly. It is worth mentioning that form factors at large dipion invariant masses can be calculated in QCD factorization [27]. Neglecting possible resonant effects at large $\pi\pi$ invariant mass, QCD factorization provides a direct calculation of nonresonant contributions.

The nonresonant contribution in the π^-K^+ system is given by

$$A_{\mathrm{NR}}^{\pi^-K^+} = \langle K^-(p_3)|\bar{s}b|B^-\rangle\langle\pi^-(p_1)$$
$$\times K^+(p_2)|\bar{d}s|0\rangle^{\mathrm{NR}}(-2a_6^p + a_8^p)$$
$$= \frac{m_B^2 - m_K^2}{m_b - m_s}F_0^{BK}(s_{12})\langle\pi^-(p_1)$$
$$\times K^+(p_2)|\bar{d}s|0\rangle^{\mathrm{NR}}(-2a_6^p + a_8^p), \quad (2.22)$$

where the nonresonant matrix element of scalar density has the expression [9,10]

$$\langle\pi^-(p_1)K^+(p_2)|\bar{d}s|0\rangle^{\mathrm{NR}} = \sigma_{\mathrm{NR}}e^{-\alpha s_{12}}\left(1 - 4\frac{m_K^2 - m_\pi^2}{s_{12}}\right),$$
$$(2.23)$$

with[4]

$$\sigma_{\mathrm{NR}} = e^{i\phi_{\pi K}}(4.74_{-0.29}^{+0.25}) \text{ GeV}, \qquad \alpha = 0.069 \text{ GeV}^{-2},$$
$$(2.24)$$

where the phase $\phi_{\pi K}$ will be specified later. As stressed in [10], the nonresonant signal in the π^-K^+ system is governed by the nonresonant component of the matrix

---

[3]The parameter $\alpha_{\mathrm{NR}} = 0.081_{-0.009}^{+0.015}$ GeV^{-2} used in [9,10] was originally constrained from the *BABAR*'s measurement of the nonresonant contribution to $B^- \to \pi^+\pi^-\pi^-$ [7]. However, a substantial part of the nonresonant amplitude is now replaced by the scalar σ meson in the LHCb analysis based on the isobar model. This leads to a larger α_{NR}.

[4]The value of the parameter σ_{NR} given in [8] was determined at the scale $\mu = \bar{m}_b/2$. In this work, we will confine ourselves to the renormalization scale $\mu = \bar{m}_b(\bar{m}_b) = 4.18$ GeV, see also Appendix B. In our previous work [9,10] we employed the *BABAR* measurement $\alpha = (0.14 \pm 0.02)$ GeV^{-2} [31]. In order to fit to the nonresonant rate in the π^-K^+ system, the value of α is reduced by a factor of 2.

element of scalar density. Owing to the exponential suppression factor $e^{-\alpha s_{12}}$, the nonresonant contribution manifests in the low invariant mass regions. Note that in the LHCb analysis, the nonresonant amplitude is parametrized in terms of a simple single-pole form factor of the type $(1 + m^2_{\pi^\pm K^\mp}/\Lambda^2)^{-1}$ with $\Lambda \sim 1$ GeV. We prefer to use the exponential form for nonresonant amplitudes.

C. Final-state rescattering

CP asymmetries (integrated or regional) measured by the LHCb are positive for $h^-\pi^+\pi^-$ and negative for $h^-K^+K^-$ with $h = \pi$ or K. The former usually has a larger CP asymmetry in magnitude than the latter. This has led to the conjecture that $\pi^+\pi^- \leftrightarrow K^+K^-$ rescattering may play an important role in the generation of the strong phase difference needed for such a violation to occur [3]. The CPT theorem requires that $\Delta\Gamma^{\rm FSI}_\lambda \equiv \Gamma(B \to \lambda)^{\rm FSI} - \Gamma(\bar{B} \to \bar{\lambda})^{\rm FSI}$ be vanished when summing over all the possible states allowed by final-state interactions; that is, $\sum_\lambda \Delta\Gamma^{\rm FSI}_\lambda = 0$. However, in the LHCb analysis, only the two channels $\alpha = \pi^+\pi^- P^-$ and $\beta = K^+K^- P^-$ ($P = \pi, K$) in B^- decays are assumed to be strongly coupled through final-state interactions with the third meson P being treated as a bachelor or a spectator. It follows that $\Delta\Gamma^{\rm FSI}_\beta = -\Delta\Gamma^{\rm FSI}_\alpha$. It was found that final-state rescattering of $\pi^+\pi^- \leftrightarrow K^+K^-$ dominates the asymmetry in the mass region between 1 and 1.5 GeV. In reality, the consideration of only rescattering between $\pi^+\pi^-$ and K^+K^- in the S-wave configuration is too restrictive and simplified [32]. For example, $\pi^+\pi^-$ is allowed to rescatter into K^+K^- with charge neutral multipion states. Nevertheless, below we shall follow the work of [33] (also the same framework adapted in [34]) to describe the inelastic $\pi\pi \leftrightarrow K\bar{K}$ rescattering process and consider this final-state rescattering effect on inclusive and local CP violation.

Neglecting possible interactions with the third meson under the so-called "2 + 1" assumption, the S-wave $\pi^+\pi^- \leftrightarrow K^+K^-$ rescattering through final-state interactions is described by [35,36][5]

$$
\begin{pmatrix} A(B^- \to \pi^+\pi^- P^-) \\ A(B^- \to K^+K^- P^-) \end{pmatrix}^{\rm FSI}_{S\text{-wave}}
$$
$$
= S^{1/2} \begin{pmatrix} A(B^- \to \pi^+\pi^- P^-) \\ A(B^- \to K^+K^- P^-) \end{pmatrix}_{S\text{-wave}} \quad (2.25)
$$

with $P = \pi, K$. The unitary S matrix reads

$$
S = \begin{pmatrix} \eta e^{2i\delta_{\pi\pi}} & i\sqrt{1-\eta^2}e^{i(\delta_{\pi\pi}+\delta_{K\bar{K}})} \\ i\sqrt{1-\eta^2}e^{i(\delta_{\pi\pi}+\delta_{K\bar{K}})} & \eta e^{2i\delta_{K\bar{K}}} \end{pmatrix}, \quad (2.26)
$$

---

[5]This is different from our previous treatment in [10] in one aspect, namely, only the S-wave $\pi\pi$ and $K\bar{K}$ amplitudes will undergo final-state rescattering.

where the inelasticity parameter $\eta(s)$ is given by [33]

$$
\eta(s) = 1 - \left(\epsilon_1 \frac{k_2}{s^{1/2}} + \epsilon_2 \frac{k_2^2}{s}\right) \frac{M'^2 - s}{s}, \quad (2.27)
$$

with

$$
k_2 = \frac{\sqrt{s - 4m^2_{K(\pi)}}}{2} \quad (2.28)
$$

for rescattering to a pair of kaons (pions). The $\pi\pi$ phase shift has the expression

$$
\delta_{\pi\pi}(s) = \frac{1}{2}\cos^{-1}\left(\frac{\cot^2[\delta_{\pi\pi}(s)] - 1}{\cot^2[\delta_{\pi\pi}(s)] + 1}\right), \quad (2.29)
$$

with

$$
\cot[\delta_{\pi\pi}(s)] = c_0 \frac{(s - M_s^2)(M_f^2 - s)}{M_f^2 s^{1/2}} \frac{|k_2|}{k_2^2}. \quad (2.30)
$$

We shall assume that $\delta_{K\bar{K}} \approx \delta_{\pi\pi}$ in the rescattering region. We have shown in [10] that the matrix $S^{1/2}$ can be expressed as

$$
S^{1/2} = e^{i\delta_{\pi\pi}}\begin{pmatrix} \cos\phi/2 & i\sin\phi/2 \\ i\sin\phi/2 & \cos\phi/2 \end{pmatrix}, \quad (2.31)
$$

with

$$
\phi = \tan^{-1}\frac{\sqrt{1-\eta^2}}{\eta}. \quad (2.32)
$$

For numerical calculations we shall use the parameters given in Eqs. (2.15b') and (2.16) of [33], namely $M' = 1.5$ GeV, $M_s = 0.92$ GeV, $M_f = 1.32$ GeV, $\epsilon_1 = 2.4$, $\epsilon_2 = -5.5$, and $c_0 = 1.3$.

The rescattering amplitude reads from Eqs. (2.25) and (2.31) to be

$$
A(B^- \to K^+K^-\pi^-)_{\rm rescattering}
$$
$$
= e^{i\delta_{\pi\pi}}[\cos(\phi/2)A(B^- \to K^+K^-\pi^-)_{S\text{-wave}}
$$
$$
+ i\sin(\phi/2)A(B^- \to \pi^+\pi^-\pi^-)_{S\text{-wave}}]. \quad (2.33)
$$

The S-wave amplitudes involved in rescattering are given by

$$
A(B^- \to K^+K^-\pi^-)_{S\text{-wave}} = A^{K^+K^-}_{\rm NR} + A_{f_0(980)},
$$
$$
A(B^- \to \pi^+\pi^-\pi^-)_{S\text{-wave}} = A^{\pi^+\pi^-}_{\rm NR} + A_{\sigma(500)}. \quad (2.34)
$$

The nonresonant amplitude $A^{\pi^+\pi^-}_{\rm NR}$ and the amplitude with the scalar resonance $\sigma(500)$ will be discussed in Sec. III.

Equation (2.25) is sometimes expressed in the literature in terms of the S matrix instead of $S^{1/2}$. For example, writing the decay amplitude as $\mathcal{A}^{\pm} = A_{\lambda} + B_{\lambda}e^{\pm i\gamma}$, it has been shown in [34] that the lowest-order (LO) effect due to FSI in the decay amplitude is given by (see Eq. (18) of [34])

$$\mathcal{A}_{\text{LO}}^{\pm} = A_{0\lambda} + e^{\pm i\gamma}B_{0\lambda} + i\sum_{\lambda'}t_{\lambda',\lambda}(A_{0\lambda'} + e^{\pm i\gamma}B_{0\lambda'})$$
$$\to \sum_{\lambda'}S_{\lambda,\lambda'}(A_{0\lambda'} + e^{\pm i\gamma}B_{0\lambda'}), \quad (2.35)$$

where use of $S_{ij} = S_{ji}$ has been made. However, the reader can check that the above amplitude does not satisfy Eq. (12) of [34] up to the leading order in $t_{\lambda',\lambda}$, namely,

$$A_{\lambda} + e^{\mp i\gamma}B_{\lambda} = \chi_h\chi_{\lambda}(A_{\lambda} + e^{\pm i\gamma}B_{\lambda})^*$$
$$+ i\chi_h\chi_{\lambda}\sum_{\lambda'}t_{\lambda',\lambda}(A_{\lambda'} + e^{\pm i\gamma}B_{\lambda'})^*, \quad (2.36)$$

with the relations $A_{0\lambda} = \chi_h\chi_{\lambda}A_{0\lambda}^*$ and $B_{0\lambda} = \chi_h\chi_{\lambda}B_{0\lambda}^*$. The correct answer should read

$$\mathcal{A}_{\text{LO}}^{\pm} = A_{0\lambda} + e^{\pm i\gamma}B_{0\lambda} + \frac{i}{2}\sum_{\lambda'}t_{\lambda,\lambda'}(A_{0\lambda'} + e^{\pm i\gamma}B_{0\lambda'})$$
$$\to \sum_{\lambda'}S_{\lambda,\lambda'}^{1/2}(A_{0\lambda'} + e^{\pm i\gamma}B_{0\lambda'}). \quad (2.37)$$

Hence, Eq. (2.25) gives the correct description of $\pi^+\pi^- \leftrightarrow K^+K^-$ final-state rescattering.[6] However, the LHCb

analysis of $\pi\pi \leftrightarrow K\bar{K}$ rescattering is based on the model described in [34,39].

D. Numerical results and discussions

The total decay amplitude of $B^- \to \pi^-K^+K^-$ now reads

$$A(B^- \to \pi^-K^+K^-)$$
$$= \frac{G_F}{\sqrt{2}}\sum_{p=u,c}\lambda_p(A_{K^*(892)} + A_{K_0^*(1430)} + A_{f_0(980)} + A_{\phi(1020)}$$
$$+ A_{\rho(1450)} + A_{f_2(1270)} + A_{\text{NR}}^{\pi^-K^+} + A_{\text{NR}}^{K^+K^-} + A_{\text{rescattering}}), \quad (2.38)$$

with $\lambda_p \equiv V_{pb}V_{pd}^*$.

The strong coupling constants such as $g^{K^{*0}\to\pi^-K^+}$ and $g^{f_0(980)\to K^+K^-}, \cdots$ etc., are determined from the measured partial widths through the relations[7]

$$\Gamma_{S\to P_1P_2} = \frac{p_c}{8\pi m_S^2}g_{S\to P_1P_2}^2,$$

$$\Gamma_{V\to P_1P_2} = \frac{p_c^3}{6\pi m_V^2}g_{V\to P_1P_2}^2,$$

$$\Gamma_{T\to P_1P_2} = \frac{p_c^5}{60\pi m_T^2}g_{T\to P_1P_2}^2, \quad (2.39)$$

for scalar, vector and tensor mesons, respectively, where p_c is the c.m. momentum. Numerically, they are given by

$$|g^{\rho(770)\to\pi^+\pi^-}| = 6.00,$$
$$|g^{\phi\to K^+K^-}| = 4.54,$$
$$|g^{f_0(980)\to\pi^+\pi^-}| = 1.33_{-0.26}^{+0.29} \text{ GeV},$$
$$|g^{K_0^*(1430)\to K^+\pi^-}| = 3.84 \text{ GeV},$$
$$|g^{f_2(1270)\to\pi^+\pi^-}| = 18.56 \text{ GeV}^{-1},$$

$$|g^{K^*(892)\to K^+\pi^-}| = 4.59,$$
$$|g^{\omega\to\pi^+\pi^-}| = 0.18,$$
$$|g^{f_0(980)\to K^+K^-}| = 3.70 \text{ GeV},$$
$$|g^{\sigma\to\pi^+\pi^-}| = 2.76 \text{ GeV},$$
$$|g^{f_2(1270)\to K^+K^-}| = 11.11 \text{ GeV}^{-1}, \quad (2.40)$$

---

[6]In Eq. (2.25) we have used the factorized amplitude $\mathcal{A}_{\text{fac}}$ in the place of $A_{0\lambda'} + e^{\pm i\gamma}B_{0\lambda'}$. They are, however, not exactly the same. In fact, we are using a time evolution picture [37,38] and the rescattering of $\pi\pi \to K\bar{K}$ happens at a much later stage of time-evolution. The full amplitude should read $\mathcal{A} = \mathcal{S}^{1/2}\mathcal{A}_0$ with $\mathcal{A}_0$ being free from any strong phase, and the S-matrix $\mathcal{S}^{1/2}$ corresponds to a time-evolution operator $U(\infty, 0)$ [37] (see Appendix C for details). Then we separate the time-evolution operator into $U(\infty, 0) = U(\infty, \tau)U(\tau, 0)$ with τ being short enough to treat quarks and gluons as good degrees of freedom. Consequently, the strong phase in $U(\tau, 0)\mathcal{A}_0$ can be calculated in the factorization approach giving $\mathcal{A}_{\text{fac}} = U(\tau, 0)\mathcal{A}_0$ [35,38]. Hence, the full amplitude becomes $\mathcal{A} = U(\infty, \tau)\mathcal{A}_{\text{fac}}$, which corresponds to Eq. (2.25) with $\pi\pi \to K\bar{K}$ rescattering contained in $U(\infty, \tau) = S^{1/2}$.

[7]There is some confusion in the literature concerned with the relation between the width and coupling for the tensor meson. For example, it was expressed as $\Gamma_{T\to P_1P_2} = \alpha_{TP_1P_2}\frac{p_c^5}{60\pi m_T^2}g_{T\to P_1P_2}^2$ [40], where the factor of $\alpha_{TP_1P_2}$ takes into account the average over spin of the initial state and sum over final isospin states with averaging over initial isospin states, while the relation $\Gamma_{T\to P_1P_2} = \frac{p_c^5}{15\pi m_T^2}g_{T\to P_1P_2}^2$ was used in [41,42]. It turns out that the narrow width approximation, for instance, $\Gamma(B^+ \to f_2\pi^+ \to \pi^+\pi^-\pi^+) = \Gamma(B^+ \to f_2\pi^+)\mathcal{B}(f_2 \to \pi^+\pi^-)$ is respected if the tensor coupling and width satisfy the relation given in Eq. (2.39).

where we have used $\Gamma(f_0(980) \to \pi^+\pi^-) = (34.2^{+13.9+8.8}_{-11.8-2.5})$ MeV [43], $m_\sigma = 563$ MeV and $\Gamma_\sigma = 350$ MeV obtained in the isobar model fit by the LHCb [6]. Note that the strong coupling constant is determined up to a strong phase ambiguity, for example, the strong coupling $g^{\sigma \to \pi^+\pi^-}$ has the expression

$$g^{\sigma \to \pi^+\pi^-} = |g^{\sigma \to \pi^+\pi^-}|e^{i\phi_\sigma}. \tag{2.41}$$

Below we will use this freedom of the strong phase ϕ_σ to accommodate a large negative CP asymmetry through $\pi^+\pi^- \to K^+K^-$ rescattering.

As for the $\rho(1450)$ meson, there is no any experimental information for its decays to K^+K^- and $\pi^+\pi^-$ except for the ratio

$$R_{\rho(1450)} \equiv \frac{\mathcal{B}(\rho(1450)^0 \to K^+K^-)}{\mathcal{B}(\rho(1450)^0 \to \pi^+\pi^-)}$$
$$= 0.307 \pm 0.084 \pm 0.082, \tag{2.42}$$

measured by *BABAR* through the decay $J/\psi \to h^+h^-\pi^0$ [44]. Nevertheless, we can use the measured fractions of $B^- \to \rho(1450)\pi^- \to \pi^+\pi^-\pi^-$ and $K^+K^-\pi^-$ by LHCb and the partial widths of $B^- \to \pi^+\pi^-\pi^-$ and $B^- \to K^+K^-\pi^-$ to extract the strong couplings. Assuming the same B–$\rho(1450)$ transition form factors as that of B–$\rho(770)$ ones, we obtain

$$g^{\rho(1450)\to K^+K^-} = 5.40, \qquad g^{\rho(1450)\to \pi^+\pi^-} = 2.31. \tag{2.43}$$

Contrary to the naive expectation, $\rho(1450)$ couples more strongly to K^+K^- than $\pi^+\pi^-$. This is not consistent with the *BABAR*'s measurement given in Eq. (2.42). Since

$$R_{\rho(1450)} = \left(\frac{g^{\rho(1450)\to K^+K^-}}{g^{\rho(1450)\to \pi^+\pi^-}}\right)^2 \left(\frac{m^2_{\rho(1450)} - 4m^2_K}{m^2_{\rho(1450)} - 4m^2_\pi}\right)^{3/2}, \tag{2.44}$$

it follows that $g^{\rho(1450)\to K^+K^-}/g^{\rho(1450)\to \pi^+\pi^-} \approx 0.85$, in sharp contrast to Eq. (2.43).

As we will see in the next section, the decay $B^- \to \rho(1450)^0\pi^- \to \pi^+\pi^-\pi^-$ is well described by the pQCD approach. Hence, the issue has to do with the enormously large coupling of $\rho(1450)$ with $K\bar{K}$. Indeed, a recent study in [45] showed that the pQCD prediction for the branching fraction of $B^+ \to \pi^+\rho(1450)^0 \to \pi^+K^+K^-$ is about 18 times smaller than experiment. Note that both *BABAR* and Belle used to see a broad scalar resonance $f_X(1500)$ in $B \to K^+K^+K^-$, $K^+K^-K_S$, and $K^+K^-\pi^+$ decays at energies around 1.5 GeV. However, the nature of $f_X(1500)$ is not clear as it cannot be identified with the well known scaler meson $f_0(1500)$. An angular-momentum analysis of the above-mentioned three channels by *BABAR* [46] showed that the $f_X(1500)$ state is not a single scalar resonance, but instead can be described by the sum of the well-established resonances $f_0(1500)$, $f_0(1710)$ and $f'_2(1525)$. Since $\rho(1450)$ is very board with a width 400 ± 60 MeV [47], a broad vector resonance $\rho_X(1500)$ instead of the scalar one $f_X(1500)$ is an interesting possibility to describe the broad resonance observed at energies ~ 1.5 GeV in $B \to KKK$ and $K\bar{K}\pi$ decays.

The calculated branching fractions of resonant and nonresonant contributions to $B^- \to \pi^-K^+K^-$ are summarized in Table II. The theoretical errors arise from the uncertainties in (i) form factors and the strange quark mass m_s, (ii) the unitarity angle γ and (iii) the parameter σ_{NR} [see Eq. (2.24)] which governs the nonresonant matrix elements of scalar densities.

TABLE II. Branching fractions (in units of 10^{-6}) and CP violation of various contributions to $B^\pm \to \pi^\pm K^+K^-$ decays. The experimental branching fraction of each contribution is inferred from the measured fit fraction [4] together with the world average $\mathcal{B}(B^\pm \to \pi^\pm K^+K^-) = (5.24 \pm 0.42) \times 10^{-6}$ [48], for example, $\mathcal{B}(B^- \to K^*(890)^0K^- \to K^+\pi^-K^-) = (0.39 \pm 0.05) \times 10^{-6}$. For rescattering contributions, we consider two cases for the S-wave $\pi\pi \to K\bar{K}$ transition amplitudes: Eq. (2.51) for case (i) and Eq. (2.52) for case (ii).

Contribution	$\mathcal{B}_{\text{expt}}$	$\mathcal{B}_{\text{theory}}$	$(\mathcal{A}_{CP})_{\text{expt}}(\%)$	$(\mathcal{A}_{CP})_{\text{theory}}(\%)$
$K^*(890)^0$	0.39 ± 0.05	$0.23^{+0.04}_{-0.04}$	12.3 ± 9.8	$-23.7^{+0.2}_{-0.2}$
$K^*_0(1430)^0$	0.23 ± 0.08	$0.71^{+0.13}_{-0.12}$	10.4 ± 17.3	$-19.9^{+0.1}_{-0.1}$
$\rho(1450)^0$	1.61 ± 0.15	Fit	-10.9 ± 5.0	$11.4^{+0.3}_{-0.4}$
$f_2(1270)$	0.39 ± 0.06	$0.05^{+0.01}_{-0.01}$	26.7 ± 11.3	$24.9^{+0.1}_{-0.1}$
$\phi(1020)$	0.016 ± 0.008	$0.0079^{+0.0019}_{-0.0017}$	9.8 ± 51.1	0
$f_0(980)$	$\cdots$	$0.19^{+0.03}_{-0.03}$	$\cdots$	$15.1^{+0.4}_{-0.5}$
NR$(\pi^\pm K^\mp)$	1.69 ± 0.27	$1.68^{+0.43}_{-0.39}$	-10.7 ± 6.4	$-17.8^{+0.1}_{-0.1}$
NR(K^+K^-)	$\cdots$	$0.14^{+0.05}_{-0.06}$	$\cdots$	$-2.89^{+0.02}_{-0.02}$
Rescattering	0.85 ± 0.10	(i) $0.75^{+0.21}_{-0.18}$	-66.4 ± 4.2	Fit
		(ii) $0.20^{+0.06}_{-0.05}$	-66.4 ± 4.2	Fit

1. $\phi(1020)$ production

The $\phi(1020)$ production proceeds through the $b \to d$ penguin diagram. Its signature is very small due to the smallness of the penguin coefficients $a_{3,5,7,9}$, see Eq. (2.25). Indeed, the branching fraction of the quasi-two-body decay $B^- \to \phi\pi^-$ is expected to be very small, of order 4.3×10^{-8} [49]. It is induced mainly from $B^- \to \omega\pi^-$ followed by a small $\omega - \phi$ mixing. A recent pQCD calculation yields $\mathcal{B}(B^- \to \phi(1020)\pi^+ \to K^+K^-\pi^-) = (3.59 \pm 1.17 \pm 1.87 \pm 0.34) \times 10^{-9}$ [50], to be compared with ours $(7.9^{+1.9}_{-1.7}) \times 10^{-9}$.

2. $K_0^*(1430)$ contribution

We see from Table II that the $K_0^*(1430)^0$ contribution to $B^- \to K^+K^-\pi^-$ is larger than experiment by a factor of 3. Under the narrow width approximation

$$\mathcal{B}(B \to RP_3 \to P_1P_2P_3) = \mathcal{B}(B \to RP_3)\mathcal{B}(R \to P_1P_2),$$
$$(2.45)$$

the branching fraction[8]

$$\mathcal{B}(B^- \to K_0^*(1430)^0 K^-) = (0.38 \pm 0.12 \pm 0.05) \times 10^{-6}$$
$$(2.46)$$

is obtained by the PDG [47]. This mode has been studied in both pQCD and QCDF approaches with the predictions

$$\mathcal{B}(B^- \to K_0^*(1430)^0 K^-) \times 10^6 = 1.2^{+0.2+0.1+0.1+0.2}_{-0.1-0.1-0.1-0.2} \,(S1),$$
$$2.2^{+0.6+0.2+0.4+0.5}_{-0.4-0.2-0.1-0.4} \,(S2), \qquad (2.47)$$

in pQCD [51] and

$$\mathcal{B}(B^- \to K_0^*(1430)^0 K^-) \times 10^7 = 23.71^{+6.67+6.73+2.61}_{-5.60-4.61-3.64} \,(S1),$$
$$33.70^{+10.33+5.52+3.37}_{-8.47-4.82-3.94} \,(S2), \qquad (2.48)$$

in QCDF [52], where S1 and S2 denote two different scenarios for the quark content of the scalar meson. All scalar mesons are made of $q\bar{q}$ quarks in scenario 1, while in scenario 2 the scalar mesons above 1 GeV are lowest-lying $q\bar{q}$ scalar states and the light scalar mesons are four-quark states. As discussed in [53,54], scenario 2 is preferable. It appears that the current theoretical predictions for $\mathcal{B}(B^- \to K_0^*(1430)^0 K^-)$ are too large compared to experiment. This issue needs to be resolved. It is interesting to notice that the predicted $K_0^*\pi$ rates in $B \to K\pi\pi$ decays are usually *smaller* than the results obtained by *BABAR* and Belle, see Table VI of [9]. For example, the calculated branching fraction of $\bar{K}_0^{*0}(1430)\pi^-$ in $B^- \to K^-\pi^+\pi^-$ is smaller than the *BABAR* measurement by a factor of two and the Belle result by a factor of three. As discussed in detail in [9], *BABAR* and Belle have different definitions for the $K_0^*(1430)$ and nonresonant components.

3. $f_2(1270)$

The calculated branching fraction for $f_2(1270)$ is smaller than experiment by a factor of ~ 7 in its central value. We have used the form factor $A_0^{Bf_2(1270)}(0) = 0.13 \pm 0.02$ derived from large energy effective theory (see Table II of [19]). Notice that the same form factor leads to a prediction of $\mathcal{B}(B^- \to f_2(1270)\pi^- \to \pi^+\pi^-\pi^-)$ consistent with the experimental value (see Table VI). Using the narrow width approximation (2.45) and the branching fractions of $f_2(1270)$ [47]

$$\mathcal{B}(f_2(1270) \to K^+K^-) = \frac{1}{2} \times (0.046^{+0.005}_{-0.004}),$$
$$\mathcal{B}(f_2(1270) \to \pi^+\pi^-) = \frac{2}{3} \times (0.842^{+0.029}_{-0.009}), \qquad (2.49)$$

it is straightforward to obtain

$$\mathcal{B}(B^- \to f_2(1270)\pi^-) = \begin{cases} (17.1 \pm 3.2) \times 10^{-6} & \text{from } B^- \to f_2(1270)\pi^- \to K^+K^-\pi^- \\ (2.4 \pm 0.5) \times 10^{-6} & \text{from } B^- \to f_2(1270)\pi^- \to \pi^+\pi^-\pi^-, \end{cases} \qquad (2.50)$$

where the rates of $B^- \to f_2(1270)\pi^- \to K^+K^-\pi^-$ and $B^- \to f_2(1270)\pi^- \to \pi^+\pi^-\pi^-$ are shown in Tables II and VI, respectively. Evidently, $\mathcal{B}(B^- \to f_2(1270)\pi^-)$ extracted from two different processes differs by a factor of seven. This implies that the $f_2(1270)$ contribution to

---

[8]Since $K_0^*(1430)$ with a width 270 ± 80 MeV is not so narrow, the narrow width approximation is not fully justified and presumably finite-width effects need to be taken into account to extract the branching fraction of $B^- \to K_0^*(1430)^0 K^-$.

$B^- \to K^+K^-\pi^-$ is probably largely overestimated experimentally. Indeed, $B^- \to f_2(1270)\pi^-$ is predicted to have the branching fraction of $(2.7^{+1.4}_{-1.2}) \times 10^{-6}$ in the QCDF approach [19]. This issue needs to be clarified in the Run II experiment. (iv) The predicted *CP* asymmetry of 25% in the $f_2(1270)$ component agrees with the measured value, though the experimental signature for *CP* violation is only 2.4σ. Nevertheless, a large *CP* asymmetry is clearly observed in the process of $B^- \to f_2(1270)\pi^- \to \pi^+\pi^-\pi^-$ to be discussed in Sec. III.

4. Nonresonant contributions

Although the nonresonant contribution in the K^+K^- system was not considered by the LHCb, our calculation shown in Table II indicates that it is very suppressed relative to the nonresonant one in the π^-K^+ system. This is contrary to the previous expectation that the dominant nonresonant contributions for tree-dominated three-body decays arise from the $b \to u$ tree transition rather than from the penguin amplitude process. We have identified the nonresonant contribution in the $\pi^\pm K^\mp$ system with the matrix element of scalar density $\langle\pi^-K^+|\bar{d}s|0\rangle^{\mathrm{NR}}$. The values of the NR parameters α_{NR}, σ_{NR} and α in Eqs. (2.21) and (2.24) have been modified in this work.

5. CP violation via rescattering

From Eqs. (2.33) and (2.34), the S-wave $\pi^+\pi^- \to K^+K^-$ transition amplitude reads

$$ie^{i\delta_{\pi\pi}}\sin(\phi/2)(A_{\mathrm{NR}}^{\pi^+\pi^-} + A_\sigma). \tag{2.51}$$

Recall that the phase ϕ_σ of the coupling $g^{\sigma\to\pi^+\pi^-}$ is unknown [see Eq. (2.41)]. By varying ϕ_σ or the relative phase between A_σ and $A_{\mathrm{NR}}^{\pi^+\pi^+}$, we find that a large CP asymmetry of -66% can be accommodated at $\phi_\sigma \approx 134°$. The branching fraction is $(0.20^{+0.06}_{-0.05}) \times 10^{-6}$ as shown in

Table II. Since the LHCb analysis of $\pi\pi \leftrightarrow K\bar{K}$ rescattering is based on the model described in [34,39], the S-wave transition amplitude in this case is given by

$$ie^{2i\delta_{\pi\pi}}\sqrt{1-\eta^2}(A_{\mathrm{NR}}^{\pi^+\pi^-} + A_\sigma). \tag{2.52}$$

The observed CP asymmetry is fitted with the same phase $\phi_\sigma = 134°$, but the corresponding branching fraction becomes $(0.75^{+0.21}_{-0.18}) \times 10^{-6}$. This is consistent with the experimental value of $(0.85 \pm 0.10) \times 10^{-6}$. Note that the calculated rate for rescattering differs by a factor of ~ 4 as the transition amplitude is different by a factor of two to the leading order of $t_{\lambda,\lambda'}$ [see Eqs. (2.35) and (2.37)]. Nevertheless, we have stressed in passing that one should use Eq. (2.25) to describe $\pi\pi \leftrightarrow K\bar{K}$ final-state rescattering. Therefore, the branching fraction of the rescattering contribution seems to be overestimated by the LHCb by a factor of 4.

6. Inclusive and local CP asymmetries

The inclusive CP asymmetry $\mathcal{A}_{CP}^{\mathrm{incl}}$ in $B^- \to K^+K^-\pi^-$ has been measured at B factories and LHCb with the results: $0.00 \pm 0.10 \pm 0.03$ by *BABAR* [14], $(-17.0 \pm 7.3 \pm 1.7)\%$ by Belle [15] and $(-12.3 \pm 1.7 \pm 1.2 \pm 0.7)\%$ by LHCb [2]. The world average is $\mathcal{A}_{CP}^{\mathrm{incl}} = -0.122 \pm 0.021$ [48]. Regional CP asymmetries were also measured by Belle and LHCb. The LHCb measurements read [2]

$$\mathcal{A}_{CP}^{\mathrm{low}} = (-64.8 \pm 7.0 \pm 1.3 \pm 0.7)\% \quad \text{for } m_{K^+K^-} < 1.22 \text{ GeV},$$
$$\mathcal{A}_{CP}^{\mathrm{resc}} = (-32.8 \pm 2.8 \pm 2.9 \pm 0.7)\% \quad \text{in } 1.0 < m_{K^+K^-} < 1.5 \text{ GeV}, \tag{2.53}$$

while Belle found [15]

$$\mathcal{A}_{CP}^{\mathrm{local}} = \begin{cases} -0.90 \pm 0.17 \pm 0.04, & 0.8 < m_{K^+K^-} < 1.1 \text{ GeV}, \\ -0.16 \pm 0.10 \pm 0.01, & 1.1 < m_{K^+K^-} < 1.5 \text{ GeV}, \end{cases} \tag{2.54}$$

and hence a 4.8σ evidence of a negative CP asymmetry in the region $m_{K\bar{K}} < 1.1$ GeV. Note that Belle and LHCb results for local CP violation are consistent with each other.

In Table III we show the calculated inclusive and regional CP asymmetries in the presence of final-state

rescattering of S-wave $\pi^+\pi^-$ to K^+K^- and compare with experiment. Consider the phase $\phi_{\pi K}$ of the matrix element $\langle\pi^-K^+|\bar{d}s|0\rangle^{\mathrm{NR}}$ defined in Eq. (2.23). If $\phi_{\pi K}$ is set to zero, the predicted CP asymmetries $\mathcal{A}_{CP}^{\mathrm{resc}}$ and $\mathcal{A}_{CP}^{\mathrm{low}}$ will be positive, while experimentally they are negative. At first sight, this appears to be a surprise in view of a large and negative CP violation coming from rescattering. However, since the branching fraction of $\pi^+\pi^- \to K^+K^-$ transition is very small, of order 0.2×10^{-6}, its effect can be easily washed out by the presence of various resonances. Indeed, in our previous work [9,10] we have considered the case

TABLE III. Direct CP asymmetries (in %) and branching fractions of $B^\pm \to \pi^\pm K^+K^-$ decays with the superscripts denoting "incl," "resc," and "low" for CP asymmetries measured in full phase space, in the rescattering regions with $1.0 < m_{K^+K^-} < 1.5$ GeV and in the low invariant mass region where $m_{K^+K^-} < 1.22$ GeV, respectively. We consider two cases for the phase of the matrix element $\langle\pi^-K^+|\bar{d}s|0\rangle^{\mathrm{NR}}$: (i) $\phi_{\pi K} = 0$ and (ii) $\phi_{\pi K} = 250°$. Data are taken from [2] for $\mathcal{A}_{CP}^{\mathrm{low}}$, [3] for $\mathcal{A}_{CP}^{\mathrm{resc}}$, [48] for $\mathcal{A}_{CP}^{\mathrm{incl}}$ and $\mathcal{B}(B^- \to \pi^-K^+K^-)$.

	$\mathcal{A}_{CP}^{\mathrm{incl}}$	$\mathcal{A}_{CP}^{\mathrm{resc}}$	$\mathcal{A}_{CP}^{\mathrm{low}}$	$\mathcal{B}(10^{-6})$
Theory with $\phi_{\pi K} = 0$	$-0.7^{+0.9}_{-0.7}$	$13.8^{+1.3}_{-1.2}$	$15.9^{+1.1}_{-1.0}$	$4.46^{+0.95}_{-0.85}$
Theory with $\phi_{\pi K} = 250°$	$-21.9^{+1.3}_{-1.0}$	$-28.6^{+0.3}_{-0.1}$	$-51.1^{+1.6}_{-1.1}$	$5.21^{+1.14}_{-1.02}$
Expt	-12.3 ± 2.1	-32.8 ± 4.1	-64.8 ± 7.2	5.24 ± 0.42

TABLE IV.   Experimental results of the Dalitz plot fit for $B^\pm \to \pi^\pm \pi^+ \pi^-$ decays analyzed in the isobar model [5,6].

Contribution	Fit fraction (%)	$\mathcal{A}_{CP}(\%)$	B^+ phase (°)	B^- phase (°)
$\rho(770)^0$	$55.5 \pm 0.6 \pm 2.5$	$0.7 \pm 1.1 \pm 1.6$	…	…
$\omega(782)$	$0.50 \pm 0.03 \pm 0.05$	$-4.8 \pm 6.5 \pm 3.8$	$-19 \pm 6 \pm 1$	$8 \pm 6 \pm 1$
$f_2(1270)$	$9.0 \pm 0.3 \pm 1.5$	$46.8 \pm 6.1 \pm 4.7$	$5 \pm 3 \pm 12$	$53 \pm 2 \pm 12$
$\rho(1450)^0$	$5.2 \pm 0.3 \pm 1.9$	$-12.9 \pm 3.3 \pm 35.9$	$127 \pm 4 \pm 21$	$154 \pm 4 \pm 6$
$\rho_3(1690)^0$	$0.5 \pm 0.1 \pm 0.3$	$-80.1 \pm 11.4 \pm 25.3$	$-26 \pm 7 \pm 14$	$-47 \pm 18 \pm 25$
S-wave	$25.4 \pm 0.5 \pm 3.6$	$14.4 \pm 1.8 \pm 2.1$	…	…
Rescattering	$1.4 \pm 0.1 \pm 0.5$	$44.7 \pm 8.6 \pm 17.3$	$-35 \pm 6 \pm 10$	$-4 \pm 4 \pm 25$
σ	$25.2 \pm 0.5 \pm 5.0$	$16.0 \pm 1.7 \pm 2.2$	$115 \pm 2 \pm 14$	$179 \pm 1 \pm 95$

with $\phi_{\pi K} = (5/4)\pi$. As shown in Table III, the agreement between theory and experiment is greatly improved for $\phi_{\pi K} \approx 250°$. It should be stressed that although *CP* violation produced by rescattering alone is quite large, of order -66%, the regional *CP* asymmetry $\mathcal{A}_{CP}^{\text{resc}}$ will not be the same as the latter does receive contributions from other resonances.

III. $B^\pm \to \pi^\pm \pi^+ \pi^-$ DECAYS

As mentioned in the Introduction, *BABAR* has carried out the amplitude analysis of $B^- \to \pi^+ \pi^- \pi^-$ before [7]. The nonresonant S-wave fraction was measured to be $(34.9 \pm 4.2^{+8.0}_{-4.5})\%$. In the recent LHCb analysis [5,6], the S-wave component of $B^- \to \pi^+ \pi^- \pi^-$ was studied using three different approaches: the isobar model, the K-matrix model, and a quasi-model-independent (QMI) binned approach. In the isobar model, the S-wave amplitude was presented by LHCb as a coherent sum of the σ meson contribution and a $\pi\pi \leftrightarrow K\bar{K}$ rescattering amplitude in the mass range $1.0 < m_{\pi^+\pi^-} < 1.5$ GeV. The fit fraction of the S-wave is about 25% and predominated by the σ resonance (see Table IV). A large and positive *CP* asymmetry of 45% was found in the rescattering amplitude of $B^- \to \pi^+ \pi^- \pi^-$, while the corresponding *CP* violation in $B^- \to K^+ K^- \pi^-$ was of order -0.66.

Contrary to the decay $B^- \to K^+ K^- \pi^-$ where *CP* violation is observed only in the rescattering amplitude, a clear *CP* asymmetry was seen in the $B^- \to \pi^+ \pi^- \pi^-$ decay in the following places: (i) the S-wave amplitude at values of $m_{\pi^+\pi^-}$ below the mass of the $\rho(770)$ resonance, see the left panel of Fig. 1, (ii) the $f_2(1270)$ contribution, see Fig. 1 at

values of $m_{\pi^+\pi^-}$ in the $f_2(1270)$ mass region, and (iii) the interference between S- and P-waves which is clearly visible in Fig. 2 where the data are split according to the sign of $\cos\theta_{\text{hel}}$. In the isobar model, the S-wave amplitude is predominated by the σ meson. Hence, a significant *CP* violation of 15% in $B^- \to \sigma\pi^-$ is implied in this model. The significance of *CP* violation in $B^- \to f_2(1270)\pi^-$ was found to be 20σ, 15σ and 14σ for the isobar, K-matrix and QMI approaches, respectively. Therefore, *CP* asymmetry in the $f_2(1270)$ component was firmly established. As for the significance of *CP* violation in the interference between S- and P-waves exceeds 25σ in all the S-wave models.

In contrast to the above-mentioned *CP*-violating observables, *CP* asymmetry for the dominant quasi-two-body decay mode $B^- \to \rho^0 \pi^-$ was found to be consistent with zero in all three S-wave approaches (see Table V), which was already noticed by the LHCb previously in 2014 [3]. However, all the existing theoretical predictions lead to a negative *CP* asymmetry ranging from -7% to -45%. This is a long-standing puzzle [10]. In this section, we will discuss the observed *CP* violation in various modes and address the *CP* puzzle with $B^- \to \rho^0 \pi^-$.

A. Resonant contributions

The explicit expression of the factorizable tree-dominated $B^- \to \pi^-(p_1)\pi^+(p_2)\pi^-(p_3)$ decay amplitude can be found in Eq. (2.4) of [9]. Amplitudes from various resonances are listed below:

(1) $\rho(770)^0, \rho(1450)^0$

$$
\begin{aligned}
A_{\rho(770,1450)^0} = &-\frac{1}{\sqrt{2}} \frac{g^{\rho_i \to \pi^+\pi^-}}{s_{23} - m_{\rho_i}^2 + im_{\rho_i}\Gamma_{\rho_i}} (s_{12} - s_{13}) \left\{ \frac{f_\pi}{2} \left[2m_{\rho_i} A_0^{B\rho_i}(m_\pi^2) \right.\right. \\
&+ \left. \left(m_B - m_{\rho_i} - \frac{m_B^2 - s_{23}}{m_B + m_{\rho_i}} \right) A_2^{B\rho_i}(m_\pi^2) \right] [a_1 \delta_{pu} + a_4^p + a_{10}^p - (a_6^p + a_8^p)r_\chi^\pi] \\
&+ m_{\rho_i} f_{\rho_i} F_1^{B\pi}(s_{23}) \left[a_2 \delta_{pu} - a_4^p + \frac{3}{2}(a_7 + a_9) + \frac{1}{2}a_{10}^p \right] \right\} + (s_{23} \leftrightarrow s_{12}),
\end{aligned} \tag{3.1}
$$

TABLE V.   *CP* asymmetries in the quasi-two-body decay $B^- \to \rho^0(770)\pi^-$ measured by the LHCb for each *S*-wave approach [5,6].

	Isobar	*K*-matrix	QMI
$\rho(770)^0$	$0.7 \pm 1.1 \pm 0.6 \pm 1.5$	$4.2 \pm 1.5 \pm 2.6 \pm 5.8$	$4.4 \pm 1.7 \pm 2.3 \pm 1.6$

with $\rho_i = \rho(770)^0, \rho(1450)^0$. Since there are two identical π^- mesons $\pi^-(p_1)$ and $\pi^-(p_3)$ in this decay, one should take into account the identical particle effects. As a result, a factor of $\frac{1}{2}$ should be put in the decay rate.

(2) $\omega(782)$

$$
A_{\omega(782)} = -\frac{1}{\sqrt{2}} \frac{g^{\omega \to \pi^+ \pi^-}}{s_{23} - m_\omega^2 + im_\omega \Gamma_\omega} (s_{12} - s_{13}) \left\{ \frac{f_\pi}{2} \left[2m_\omega A_0^{B\omega}(m_\pi^2) \right. \right.
$$
$$
+ \left(m_B - m_\omega - \frac{m_B^2 - s_{23}}{m_B + m_\omega} \right) A_2^{B\omega}(m_\pi^2) \left] [a_1 \delta_{pu} + a_4^p + a_{10}^p - (a_6^p + a_8^p)r_\chi^\pi] \right.
$$
$$
+ m_\omega f_\omega F_1^{B\pi}(s_{23}) \left[a_2 \delta_{pu} + 2(a_3 + a_5) + a_4^p + \frac{1}{2}(a_7 + a_9 - a_{10}^p) \right] \right\} + (s_{23} \leftrightarrow s_{12}). \quad (3.2)
$$

The strong decay of $\omega(892)$ to $\pi^+ \pi^-$ is isospin-violating and it can occur through ρ–ω mixing. In this work we shall use the measured rate of $\omega \to \pi^+ \pi^-$ to fix the coupling of ω with $\pi\pi$.

(3) $f_2(1270)$

$$
A_{f_2(1270)} = \sqrt{2} \frac{m_{f_2}}{m_B} \frac{f_\pi g^{f_2 \to \pi^+ \pi^-}}{s_{23} - m_{f_2}^2 + im_{f_2}\Gamma_{f_2}} A_0^{Bf_2}(m_\pi^2) \left[\frac{1}{3} (|\vec{p}_1||\vec{p}_2|)^2 - (\vec{p}_1 \cdot \vec{p}_2)^2 \right]
$$
$$
\times [a_1 \delta_{pu} + a_4^p + a_{10}^p - (a_6^p + a_8^p)r_\chi^\pi + \beta_2^p \delta_{pu} + \beta_3^p + \beta_{3,\text{EW}}^p] + (s_{23} \leftrightarrow s_{12}), \quad (3.3)
$$

where $|\vec{p}_1|$ has the same expression as that in Eq. (2.16), but $|\vec{p}_2|$ and $|\vec{p}_3|$ are replaced by $\frac{1}{2}\sqrt{s_{23} - 4m_\pi^2}$.

(4) $\sigma/f_0(500)$

$$
A_\sigma = \frac{g^{\sigma \to \pi^+ \pi^-}}{s_{23} - m_\sigma^2 + im_\sigma \Gamma_\sigma} \left\{ -f_\pi(m_B^2 - s_{23})F_0^{B\sigma^u}(m_\pi^2)[a_1 \delta_{pu} + a_4^p + a_{10}^p - (a_6^p + a_8^p)r_\chi^\pi] \right.
$$
$$
\left. + \frac{m_\sigma}{m_b - m_d} \bar{f}_\sigma^d (m_B^2 - m_\pi^2)F_0^{B\pi}(s_{23})(-2a_6^p + a_8^p) \right\} + (s_{23} \leftrightarrow s_{12}). \quad (3.4)
$$

In the approach of QCD factorization [53,54], the decay amplitude of $B^- \to \sigma\pi^-$ has the expression

$$
A(B^- \to \sigma\pi^-) = \frac{G_F}{\sqrt{2}} \sum_{p=u,c} \lambda_p \left\{ [a_1 \delta_{pu} + a_4^p + a_{10}^p - (a_6^p + a_8^p)r_\chi^\pi]_{\sigma\pi} X^{(B\sigma,\pi)} \right.
$$
$$
+ \left[a_2 \delta_{pu} + 2(a_3^p + a_5^p) + \frac{1}{2}(a_7^p + a_9^p) + a_4^p - \frac{1}{2}a_{10}^p - \left(a_6^p - \frac{1}{2}a_8^p \right) \bar{r}_\chi^\sigma \right]_{\pi\sigma} \bar{X}^{(B\pi,\sigma)}
$$
$$
\left. - f_B f_\pi \bar{f}_\sigma^u [\delta_{pu} b_2(\pi\sigma) + b_3(\pi\sigma) + b_{3,\text{EW}}(\pi\sigma) + (\pi\sigma \to \sigma\pi)] \right\}, \quad (3.5)
$$

where

$$
X^{(B\sigma,\pi)} = -f_\pi(m_B^2 - m_\sigma^2)F_0^{B\sigma^u}(m_\pi^2), \qquad \bar{X}^{(B\pi,\sigma)} = \bar{f}_\sigma(m_B^2 - m_\pi^2)F_0^{B\pi}(m_\sigma^2), \quad (3.6)
$$

and $\bar{r}_\chi^\sigma(\mu) = 2m_\sigma/m_b(\mu)$. The order of the arguments of the $a_i^p(M_1 M_2)$ and $b_i(M_1 M_2)$ coefficients is dictated by the subscript $M_1 M_2$ given in Eq. (3.5). Note that $a_i^p(\pi\sigma)$ can be numerically very different from $a_i^p(\sigma\pi)$ except for $a_{6,8}^p$. Comparing Eqs. (3.4) and (3.5), we see that the expressions inside $\{\cdots\}$ are identical except that some terms are missing in Eq. (3.4). Those missing terms arise from vertex corrections, hard spectator interactions and penguin contractions. These subtitles are beyond the simple factorization approach adapted here.

Since the naive amplitude given by Eq. (3.4) leads to a negative *CP* asymmetry -0.015, while experimentally $\mathcal{A}_{CP}(\sigma\pi^-) = (16.0 \pm 2.8)\%$, we shall follow QCDF to keep those terms missing in the σ-emission amplitude,

$$
A_\sigma = \frac{g^{\sigma \to \pi^+\pi^-}}{s_{23} - m_\sigma^2 + im_\sigma\Gamma_\sigma} \left\{ -f_\pi(m_B^2 - s_{23})F_0^{B\sigma^u}(m_\pi^2)[a_1\delta_{pu} + a_4^p + a_{10}^p - (a_6^p + a_8^p)r_\chi^\pi]_{\sigma\pi} \right.
$$
$$
\left. + \bar{f}_\sigma^d(m_B^2 - m_\pi^2)F_0^{B\pi}(s_{23}) \left[a_2\delta_{pu} + 2(a_3^p + a_5^p) + \frac{1}{2}(a_7^p + a_9^p) + a_4^p - \frac{1}{2}a_{10}^p - \left(a_6^p - \frac{1}{2}a_8^p\right)\bar{r}_\chi^\sigma \right]_{\pi\sigma} \right\} + (s_{23} \leftrightarrow s_{12}).
$$

$$(3.7)$$

The numerical values of the flavor operators $a_i^p(M_1M_2)$ for $M_1M_2 = \sigma\pi$ and $\pi\sigma$ at the scale $\mu = \bar{m}_b(\bar{m}_b)$ are exhibited in Appendix B. It is clear that $a_i^p(\pi\sigma)$ and $a_i^p(\sigma\pi)$ can be very different numerically except for $a_{6,8}^p$.

(5) $f_0(980)$

It is straightforward to write down the amplitude for the resonance $f_0(980)$ in analog to that of $f_0(500)/\sigma$:

$$
A_{f_0(980)} = \frac{g^{f_0 \to \pi^+\pi^-}}{s_{23} - m_{f_0}^2 + im_{f_0}\Gamma_{f_0}} \left\{ X^{(Bf_0,\pi)}(m_\pi^2)[a_1\delta_{pu} + a_4^p + a_{10}^p - (a_6^p + a_8^p)r_\chi^\pi]_{f_0\pi} \right.
$$
$$
\left. + \bar{X}^{(B\pi,f_0)} \left[a_2\delta_{pu} + 2(a_3^p + a_5^p) + \frac{1}{2}(a_7^p + a_9^p) + a_4^p - \frac{1}{2}a_{10}^p - \left(a_6^p - \frac{1}{2}a_8^p\right)\bar{r}_\chi^{f_0} \right]_{\pi f_0} \right\} + (s_{23} \leftrightarrow s_{12}), \quad (3.8)
$$

with $X^{(Bf_0,\pi)}$ and $\bar{X}^{(B\pi,f_0)}$ being given by Eq. (2.7).

B. Nonresonant contributions

Just as the decay $B^- \to \pi^- K^+ K^-$, the nonresonant amplitude in the $\pi^+\pi^-$ system coming from the current-induced process through the $b \to u$ transition reads

$$
A_{\text{current-ind}}^{\text{NR}} = A_{\text{current-ind}}^{\text{HMChPT}} e^{-\alpha_{\text{NR}} p_B \cdot (p_2 + p_3)}
$$
$$
\times [a_1\delta_{pu} + a_4^p + a_{10}^p - (a_6^p + a_8^p)r_\chi^\pi], \quad (3.9)
$$

with

$$
A_{\text{current-ind}}^{\text{HMChPT}} = -\frac{f_\pi}{2}[2m_\pi^2 r + (m_B^2 - s_{23} - m_\pi^2)\omega_+
$$
$$
+ (s_{12} - s_{13})\omega_-] + (s_{23} \leftrightarrow s_{12}). \quad (3.10)
$$

Besides the current-induced one, an additional nonresonant contribution can also arise from the penguin amplitude

$$
A_{\text{penguin}}^{\text{NR}} = \langle \pi^- |\bar{d}b|B^- \rangle \langle \pi^+\pi^- |\bar{d}d|0 \rangle^{\text{NR}}(-2a_6^p + a_8^p) \quad (3.11)
$$

through the nonresonant matrix element of scalar density $\langle \pi^+\pi^- |\bar{d}d|0 \rangle^{\text{NR}}$. In our previous work, we have argued that this nonresonant background from the penguin amplitude is suppressed by the smallness of the penguin Wilson coefficients a_6 and a_8. This is no longer true in view of the very large nonresonant contribution in the $\pi^- K^+$ system of the decay $B^- \to K^+ K^- \pi^-$. The nonresonant amplitude

$$
A_{\text{NR}}^{\pi^+\pi^-} = A_{\text{current-ind}}^{\text{NR}} + A_{\text{penguin}}^{\text{NR}} \quad (3.12)
$$

is the one we used in Eq. (2.34) for describing final-state $\pi^+\pi^- \to K^+K^-$ rescattering.

C. Final-state rescattering

The rescattering amplitude reads from Eq. (2.25) to be

$$
A(B^- \to \pi^+\pi^-\pi^-)_{\text{rescattering}}
$$
$$
= e^{i\delta_{\pi\pi}}[\cos(\phi/2)A(B^- \to \pi^+\pi^-\pi^-)_{\text{S-wave}}
$$
$$
+ i\sin(\phi/2)A(B^- \to K^+K^-\pi^-)_{\text{S-wave}}], \quad (3.13)
$$

where the relevant S-wave amplitudes $A(B^- \to \pi^+\pi^-\pi^-)_{\text{S-wave}}$ and $A(B^- \to K^+K^-\pi^-)_{\text{S-wave}}$ are given in Eq. (2.34).

D. Numerical results and discussions

Using the input parameters summarized in Appendixes A and B and the amplitudes given in Sec. III A, we show the calculated results in Table VI. In the following we shall discuss each contribution in order.

1. Nonresonant component

Although nonresonant contributions were not specified in the LHCb analysis, the theoretical calculations are similar to that of $B^- \to K^+K^-\pi^-$. We find that the nonresonant background denoted by NR($\pi^+\pi^-$) in Table VI constitutes about 14% of the $B^- \to \pi^+\pi^-\pi^-$ rate and is dominated by the matrix element of scalar density

TABLE VI. Branching fractions (in units of 10^{-6}) and CP violation in various contributions to $B^{\pm} \to \pi^{\pm}\pi^+\pi^-$ decays. Experimental results are taken from the isobar model analysis [5,6]. The experimental branching fraction of each mode is inferred from the measured fit fraction [5,6] together with $\mathcal{B}(B^{\pm} \to \pi^{\pm}\pi^+\pi^-) = (15.2 \pm 1.4) \times 10^{-6}$ [7]. For rescattering contributions, we consider two cases for the S-wave $K\bar{K} \to \pi\pi$ transition amplitudes: Eq. (3.15) for case (i) and Eq. (3.16) for case (ii).

Contribution	$\mathcal{B}_{\text{expt}}$	$\mathcal{B}_{\text{theory}}$	$(\mathcal{A}_{CP})_{\text{expt}}(\%)$	$(\mathcal{A}_{CP})_{\text{theory}}(\%)$
$\rho(770)^0$	8.44 ± 0.87	$7.67^{+1.62}_{-1.47}$	0.7 ± 1.9	$11.5^{+0.3}_{-0.4}$
$\omega(782)$	0.076 ± 0.011	$0.103^{+0.024}_{-0.021}$	-4.8 ± 7.5	$-14.0^{+0.1}_{-0.1}$
$f_0(980)$	...	$0.13^{+0.02}_{-0.02}$	...	$14.7^{+0.4}_{-0.5}$
$f_2(1270)$	1.37 ± 0.26	$1.09^{+0.32}_{-0.28}$	46.8 ± 7.7	$24.9^{+0.1}_{-0.1}$
$\rho(1450)^0$	0.79 ± 0.11	Fit	-12.9 ± 36.1	$11.2^{+0.3}_{-0.4}$
$\rho_3(1690)^0$	0.076 ± 0.031	...	-80.1 ± 27.7	...
$\sigma(500)$	3.83 ± 0.84	$3.15^{+0.52}_{-0.48}$	16.0 ± 2.8	$14.9^{+0.5}_{-0.6}$
NR$(\pi^+\pi^-)$	...	$2.26^{+0.72}_{-0.61}$	...	$48.4^{+11.4}_{-13.8}$
Rescattering	0.21 ± 0.08	(i) $0.22^{+0.03}_{-0.03}$	44.7 ± 19.3	$16.3^{+0.8}_{-0.9}$
		(ii) $0.05^{+0.01}_{-0.01}$	44.7 ± 19.3	$16.3^{+0.8}_{-0.9}$

$\langle \pi^+\pi^- | \bar{d}d | 0 \rangle$. This together the σ resonance accounts for 35% of the total rate. Indeed, the nonresonant fraction was found to be 35% in the earlier *BABAR* measurement [7]. As discussed in Sec. II D 5, a large and negative CP asymmetry in the rescattering amplitude of $B^- \to \pi^- K^+ K^-$ cannot be accommodated unless the amplitude A_{σ} interferes with $A_{\text{NR}}^{\pi^+\pi^-}$.

2. $\omega(782)$

Since the $\omega(782)$ is very narrow in its width, the factorization relation for three-body decay under the narrow width approximation is expected to be valid

$$\mathcal{B}(B^- \to \omega\pi^- \to \pi^+\pi^-\pi^-) = \mathcal{B}(B^- \to \omega\pi^-)\mathcal{B}(\omega \to \pi^+\pi^-).$$
(3.14)

Using the world average $\mathcal{B}(B^- \to \omega\pi^-) = (6.9 \pm 0.5) \times 10^{-6}$ [47] and the branching fraction $\mathcal{B}(\omega \to \pi^+\pi^-) = (1.53 \pm 0.06)\%$ [47], it is expected that $\mathcal{B}(B^- \to \omega\pi^- \to \pi^+\pi^-\pi^-) = (0.106 \pm 0.009) \times 10^{-6}$. This is consistent with both theory and the LHCb measurement.

3. $f_2(1270)$

The calculated branching fraction and CP asymmetry of 25% for the process $B^- \to f_2(1270)\pi^- \to \pi^+\pi^-\pi^-$ are in accordance with experiment. Recall that the previous measurement by *BABAR* yields $\mathcal{A}_{CP}(B^- \to f_2(1270)\pi^-) = 0.41 \pm 0.25$ [7]. CP asymmetry of $(46.8 \pm 7.7)\%$ in the $f_2(1270)$ contribution was finally firmly established by the LHCb. We have shown in Eq. (2.50) two very different results of $\mathcal{B}(B^- \to f_2(1270)\pi^-)$ extracted from two different processes $B^- \to f_2(1270)\pi^- \to K^+K^-\pi^-$ and $B^- \to f_2(1270)\pi^- \to \pi^+\pi^-\pi^-$. From the latter process, *BABAR*'s measurement yields $\mathcal{B}(B^- \to f_2(1270)\pi^-) = (1.60^{+0.67+0.02}_{-0.44-0.06}) \times 10^{-6}$ [47]. This is consistent with the

result of $\mathcal{B}(B^- \to f_2(1270)\pi^-) = (2.4 \pm 0.5) \times 10^{-6}$ inferred from the LHCb [cf. Eq. (2.50)].

4. $\rho(1450)$

By considering the P-wave time-like electromagnetic form factor F_{π} for the charged pions $\pi^+\pi^-$ in the region of $\rho(1450)$ extracted from the available experimental data, the authors of [55] have studied the decay $B^- \to \rho(1450)^0\pi^- \to \pi^+\pi^-\pi^-$ within the pQCD approach. The result $\mathcal{B}(B^- \to \rho(1450)^0\pi^- \to \pi^+\pi^-\pi^-) = (8.15^{+1.46}_{-1.32}) \times 10^{-7}$ agrees well with the measured value of $(7.9 \pm 1.1) \times 10^{-7}$. However, when this approach is generalized to the P-wave time-like form factor F_K for the charged kaons K^+K^-, it appears that the calculated rate for $B^- \to \rho(1450)^0\pi^- \to K^+K^-\pi^-$ is too small compared to experiment [45]. This issue with $\rho(1450) \to K^+K^-$ needs to be resolved in the future.

5. $\sigma/f_0(500)$

Using $m_{\sigma} = 563$ MeV, $\Gamma_{\sigma} = 350$ MeV, the decay constants and form factors given in Appendix A, the decay amplitude presented in Eq. (3.7) and the flavor operators $a_i^p(M_1M_2)$ for $M_1M_2 = \sigma\pi$ and $\pi\sigma$ shown in Table IX, the resulant branching fraction $\mathcal{B}(B^- \to \sigma\pi^- \to \pi^+\pi^-\pi^-) = (3.15^{+0.52}_{-0.48}) \times 10^{-6}$ and the CP asymmetry $\mathcal{A}_{CP}(\sigma\pi^-) = (14.9^{+0.5}_{-0.6})\%$ are in good agreement with experiment (cf. Table VI). Since σ is very broad, its finite width effect which has been considered in [56] could be quite important.

6. *CP violation via rescattering*

The S-wave $K^+K^- \to \pi^+\pi^-$ transition amplitude reads from Eqs. (3.13) and (2.34) to be

$$ie^{i\delta_{\pi\pi}} \sin(\phi/2)(A_{\text{NR}}^{K^+K^-} + A_{f_0(980)}^{K^+K^-}).$$
(3.15)

Since both nonresonant contribution in the K^+K^- system and the $f_0(980)$ contribution to $B^- \to K^+K^-\pi^-$ have not been studied by the LHCb yet, we have to rely on the theoretical evaluation of these two amplitudes. The LHCb measurement of the rescattering contribution to $B^- \to \pi^+\pi^-\pi^-$ corresponds to the following transition amplitude

$$ie^{2i\delta_{\pi\pi}}\sqrt{1-\eta^2}(A_{\mathrm{NR}}^{K^+K^-} + A_{f_0(980)}^{K^+K^-}). \qquad (3.16)$$

Here we shall adapt a strategy different from that in the decay $B^- \to \pi^+\pi^-\pi^-$. We first vary the phase of the $f_0(980)K^+K^-$ coupling to fit the "measured" branching fraction and then figure out the *CP* asymmetry induced by rescattering. It turns out at $\phi_{f_0(980)} \approx 20°$, the phase of $g^{f_0(980)\to K^+K^-}$, the $K^+K^- \to \pi^+\pi^-$ transition amplitude (3.16) yields $\mathcal{B}(\text{rescattering}) = (0.22 \pm 0.03) \times 10^{-6}$ and a *CP* asymmetry of $(16.3^{+0.8}_{-0.9})\%$ (see Table VI). For the transition amplitude of Eq. (3.15), the branching fraction becomes smaller by a factor of 4, namely, $(0.05 \pm 0.01) \times 10^{-6}$. Therefore, the branching fraction of the rescattering contribution seems to be overestimated experimentally by a factor of ~ 4.

7. Inclusive and local CP asymmetries

In Table VII we show inclusive and regional *CP* asymmetries in $B^\pm \to \pi^\pm\pi^+\pi^-$ decays. The calculated $\mathcal{A}_{CP}^{\mathrm{incl}}$ and $\mathcal{A}_{CP}^{\mathrm{resc}}$ are too large compared to experiment. For a consideration of ρ–ω mixing effect on local *CP* violation, see [57].

8. CP asymmetry induced by interference

Before proceeding to discuss the *CP* asymmetry induced by interference, we follow [34] to define the quantity θ being the angle between the pions with the same-sign charge. For example, in $B^- \to \pi^-\pi^+\pi^-$ decay, it is the angle between the momenta of the two π^- pions measured in the rest frame of the dipion system (i.e., the resonance). This angle is related to the helicity angle θ_{hel} defined by the LHCb [6] through the relation $\theta_{\mathrm{hel}} + \theta = \pi$ (see Fig. 3). Hence, $\cos\theta_{\mathrm{hel}} = -\cos\theta$.

Consider the decay $B^- \to \pi^-(p_1)\pi^+(p_2)\pi^-(p_3)$ and define $s_{23} = (p_2 + p_3)^2 = m_{\pi^+\pi^-\text{low}}^2$. The angular distribution of the vector resonance is governed by the term $s_{12} - s_{13}$ [see, for example, Eq. (3.1)]. From Eq. (2.17) we have

TABLE VII. Same as Table III except for $B^\pm \to \pi^\pm\pi^+\pi^-$ decays.

	$\mathcal{A}_{CP}^{\mathrm{incl}}$	$\mathcal{A}_{CP}^{\mathrm{resc}}$	$\mathcal{A}_{CP}^{\mathrm{low}}$	$\mathcal{B}(10^{-6})$
Theory	$28.2^{+0.3}_{-0.5}$	$42.4^{+0.3}_{-0.8}$	$45.5^{+1.9}_{-2.4}$	$20.4^{+4.5}_{-3.9}$
Expt	5.8 ± 2.4	17.2 ± 2.7	58.4 ± 9.7	15.2 ± 1.4

$$s_{12} - s_{13} = -4\vec{p}_1 \cdot \vec{p}_2 = -4|\vec{p}_1||\vec{p}_2|\cos\theta_{\mathrm{hel}}$$
$$= 4\vec{p}_1 \cdot \vec{p}_3 = 4|\vec{p}_1||\vec{p}_3|\cos\theta \qquad (3.17)$$

in the rest frame of $\pi^+(p_2)$ and $\pi^-(p_3)$. As noticed in passing, $|\vec{p}_1|$ has the same expression as that in Eq. (2.16), but $|\vec{p}_2|$ and $|\vec{p}_3|$ are replaced by $\frac{1}{2}\sqrt{s_{23} - 4m_\pi^2}$. Furthermore, it follows from Eq. (3.17) that $\cos\theta$ can be expressed as a function of s_{12} and s_{23}

$$\cos\theta = a(s_{23})s_{12} + b(s_{23}), \qquad (3.18)$$

with [34]

$$a(s) = \frac{1}{(s-4m_\pi^2)^{1/2}\left(\frac{(m_B^2-m_\pi^2-s)^2}{4s} - m_\pi^2\right)^{1/2}},$$

$$b(s) = -\frac{m_B^2 + 3m_\pi^2 - s}{2(s-4m_\pi^2)^{1/2}\left(\frac{(m_B^2-m_\pi^2-s)^2}{4s} - m_\pi^2\right)^{1/2}}. \qquad (3.19)$$

For *CP* violation induced by the interference between different resonances, let us consider the low $\pi^+\pi^-$ invariant mass region of the Dalitz plot which is divided into four zones as shown in Fig. 4. The vertical line dividing zones I and III from zones II and IV is at the $\rho(770)$ mass, while the horizontal line separating zones I and II from zones III and IV is at the position where $\cos\theta = 0$, corresponding to $s_{12} = -b/a$. The cosine of the angle θ varies from -1 to 0 in zones III and IV, corresponding to $(s_{12})_{\mathrm{min}} = -(1 + b)/a$ and $s_{12} = -b/a$, respectively. Likewise, The cosine of the angle θ varies from 0 to 1 in zones I and II, corresponding to $s_{12} = -b/a$ and $(s_{12})_{\mathrm{max}} = (1-b)/a$, respectively. Hence,

$$\text{I, II}: \int_0^1 \cos\theta d\cos\theta = \int_{-b/a}^{(s_{12})_{\mathrm{max}}} (as_{12} + b)ds_{12} = \frac{1}{2},$$

$$\text{III, IV}: \int_{-1}^0 \cos\theta d\cos\theta = \int_{(s_{12})_{\mathrm{min}}}^{-b/a} (as_{12} + b)ds_{12} = -\frac{1}{2}.$$
$$(3.20)$$

In short, zones I and II are delimited by $\cos\theta > 0$ or $\cos\theta_{\mathrm{hel}} < 0$, while zones III and IV are delimited by $\cos\theta < 0$ or $\cos\theta_{\mathrm{hel}} > 0$.

The difference in the number of B^- and B^+ events measured in the low-m_{low} region for (a) $\cos\theta < 0$ (or $\cos\theta_{\mathrm{hel}} > 0$) and (b) $\cos\theta > 0$ (or $\cos\theta_{\mathrm{hel}} < 0$) is depicted in Fig. 2. In Fig. 2(a) we see that $\mathcal{A}_{CP}$ which is proportional to $N_{B^-} - N_{B^+}$ is negative below the $\rho(770)$ mass (zone III) and positive above it (zone IV) with a zero at $m_{\mathrm{low}} = m_\rho$, while in Fig. 2(b) $\mathcal{A}_{CP}$ is positive below the $\rho(770)$ mass (zone I) and negative above it (zone II). The sum of *CP* asymmetries of $\cos\theta > 0$ and $\cos\theta < 0$ gives rise to the *CP* violation shown in the left panel of Fig. 1. It is clear that *CP* asymmetry at m_{low} below the ρ mass is of order 20%,

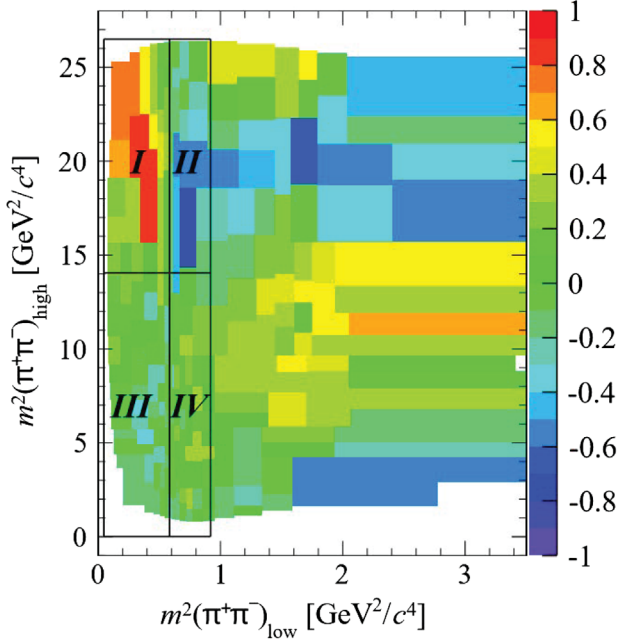FIG. 4. The low $\pi^+\pi^-$ invariant mass region of the $B^+ \to \pi^+\pi^+\pi^-$ Dalitz plot of CP asymmetries divided into four zones. This plot is taken from [58].

which is the sum of zone I and zone III. From Fig. 4 it is evident that the local CP asymmetry is largest in zone I. Indeed, LHCb has measured $\mathcal{A}_{CP}^{\rm low}(\pi^+\pi^-\pi^-)$ to be $0.584 \pm 0.082 \pm 0.027 \pm 0.007$ in the region specified by $m_{\pi^-\pi^-{\rm low}}^2 < 0.4~{\rm GeV}^2$ and $m_{\pi^+\pi^-{\rm high}}^2 > 15~{\rm GeV}^2$ [2].

In [34] the CP asymmetry of the $B^- \to \pi^+\pi^-\pi^-$ decay in the low-mass region with $s_{23} < 1~{\rm GeV}^2$ shown in Fig. 2 is described by the interference between the ρ and the nonresonant amplitude and the interference between $\rho(770)$ and $f_0(980)$ mesons. Writing

$$A_\pm \equiv A_\pm^\rho + A_\pm^{\rm NR} = c_\pm^\rho F_\rho^{\rm BW}\cos\theta + c_\pm^{\rm NR}, \qquad (3.21)$$

for the B^+ and B^- decays, where $F_\rho^{\rm BW}$ is the Breit-Wigner propagator of the $\rho(770)$

$$F_\rho^{\rm BW}(s_{23}) = \frac{1}{s_{23} - m_\rho^2 + im_\rho\Gamma_\rho}, \qquad (3.22)$$

it follows that CP asymmetry has the expression

$$\begin{aligned}\mathcal{A}_{CP} \propto & (|c_-^\rho|^2 - |c_+^\rho|^2)|F_\rho^{\rm BW}(s_{23})|^2\cos\theta^2 + (|c_-^{\rm NR}|^2 - |c_+^{\rm NR}|^2) \\ & + 2{\rm Re}(c_-^{*\rho}c_-^{\rm NR} - c_+^{*\rho}c_+^{\rm NR})|F_\rho^{\rm BW}(s_{23})|^2(s_{23} - m_\rho^2)\cos\theta \\ & + 2{\rm Im}(c_-^{*\rho}c_-^{\rm NR} - c_+^{*\rho}c_+^{\rm NR})|F_\rho^{\rm BW}(s_{23})|^2 m_\rho\Gamma_\rho\cos\theta. \end{aligned}$$
$$(3.23)$$

The terms $(s_{23} - m_\rho^2)\cos\theta$ and $m_\rho\Gamma_\rho$ arise from the imaginary and real parts, respectively, of the Breit-Wigner propagator $F_\rho^{\rm BW}$. It was argued in [34] that the first two terms violate the CPT constraint locally and will be set to zero. Assuming $c_\pm^\rho$ and $c_\pm^{\rm NR}$ are complex constants, the parameters ${\rm Re}(c_-^{*\rho}c_-^{\rm NR} - c_+^{*\rho}c_+^{\rm NR})$ and ${\rm Im}(c_-^{*\rho}c_-^{\rm NR} - c_+^{*\rho}c_+^{\rm NR})$ were obtained in [34] by fitting them to the data. The observed interference pattern in the ρ region is mainly described by the $(s_{23} - m_\rho^2)\cos\theta$ term.

Instead of fitting the unknown parameters to the data, we would like to predict the interference pattern in our approach. Since the fit fraction of the broad scalar meson σ is about 25% in the isobar model, it is natural to consider the interference between the $\rho(770)$ and $\sigma(500)$ mesons (or the broad S-wave in the other models)

$$\Gamma^{\rho-\sigma}(s_{23}) = \frac{1}{(2\pi)^3 32 m_B^3}\frac{G_F^2}{2}\frac{1}{2}\int_{(s_{12})_{\rm min}}^{-b/a} 2[{\rm Re}(A_\rho){\rm Re}(A_\sigma) + {\rm Im}(A_\rho){\rm Im}(A_\sigma)]ds_{12} \quad {\rm for}~\cos\theta < 0,$$

$$\Gamma^{\rho-\sigma}(s_{23}) = \frac{1}{(2\pi)^3 32 m_B^3}\frac{G_F^2}{2}\frac{1}{2}\int_{-b/a}^{(s_{12})_{\rm max}} 2[{\rm Re}(A_\rho){\rm Re}(A_\sigma) + {\rm Im}(A_\rho){\rm Im}(A_\sigma)]ds_{12} \quad {\rm for}~\cos\theta > 0, \qquad (3.24)$$

where the identical particle effect has been taken care of by the factor of $1/2$, and the amplitudes $A_{\rho(770)}$ and A_σ are given by Eqs. (3.1) and (3.7), respectively. The rate asymmetry $\Delta\Gamma^{\rho-\sigma} \equiv \Gamma_{B^- \to \pi^-\pi^+\pi^-} - \Gamma_{B^+ \to \pi^+\pi^+\pi^-}$ due to the $\rho(770)$ and σ interference is shown in Figs. 5(a) and 5(b) for $\cos\theta < 0$ and $\cos\theta > 0$, respectively. It is evident that the sign of CP asymmetry is flipped below and above the $\rho(770)$ peak and that the interference term is proportional to $\cos\theta$. Our calculation indicates that CP asymmetry is positive in zones I and IV, negative in zones II and III, in

agreement with the data (see Fig. 2). The interference between ρ and the nonresonant amplitude exhibits a similar feature. This interference effect is included in Figs. 5(c) and 5(d) with the rate asymmetry $\Delta\Gamma^{\rho-\sigma,\rho-{\rm NR}}$. Note that CP violation no longer vanishes exactly at $s_{23} = m_\rho^2$ due to the contributions from the imaginary part of $F_\rho^{\rm BW}$. In short, the rate asymmetry depicted in Fig. 2 is the first observation of CP violation mediated by interference between resonances with significance exceeding 25σ, though it vanishes in the $\rho(770)$ region when integrating over the angle.
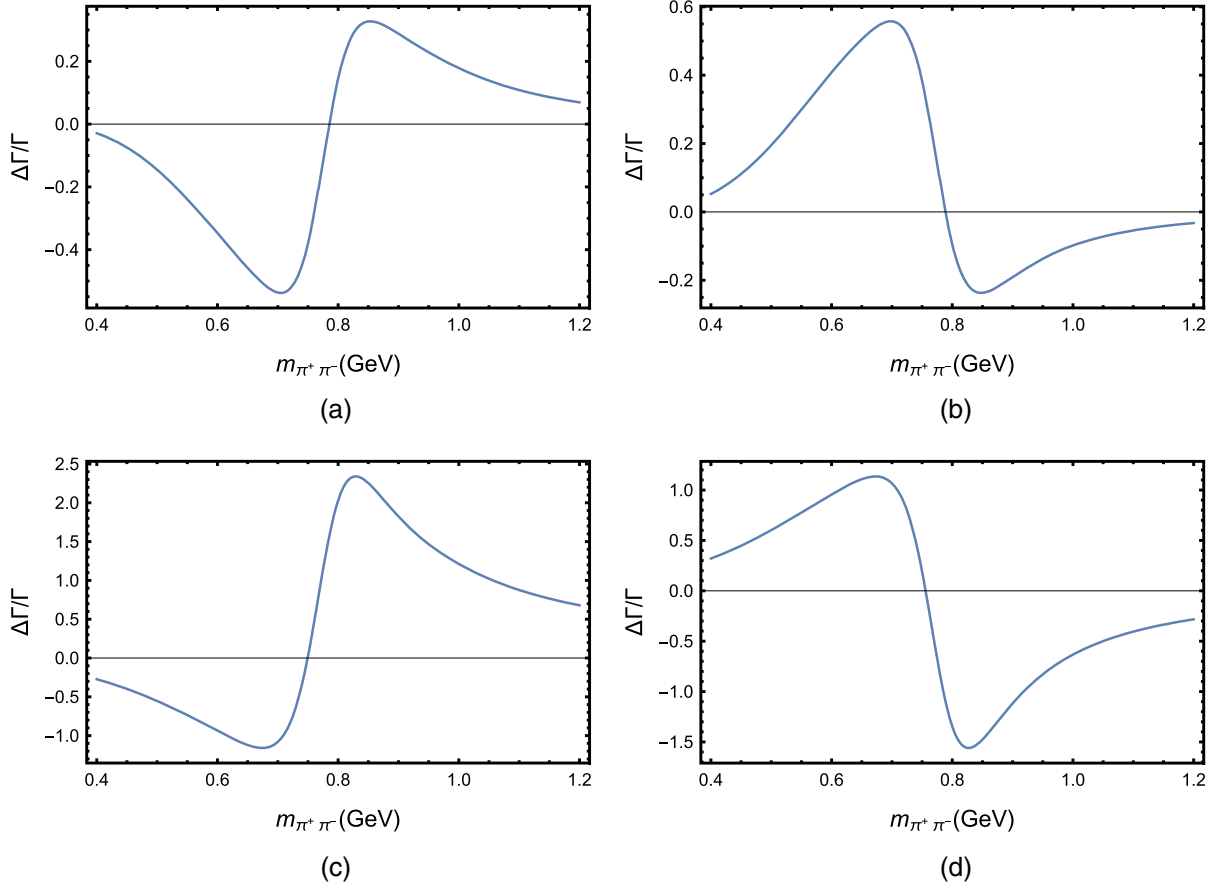
FIG. 5.   The rate asymmetry $\Delta\Gamma$ in units of $\Gamma = 1/\tau(B^{\pm})$ for $B^{\pm} \to \pi^{\pm}\pi^{+}\pi^{-}$ in the low-m_{low} region induced by the interference between $\rho(770)$ and the σ meson for (a) $\cos\theta < 0$ or $\cos\theta_{\text{hel}} > 0$ and (b) $\cos\theta > 0$ or $\cos\theta_{\text{hel}} < 0$. The interference between $\rho(770)$ and the nonresonant amplitude is added to (a) and (b) and shown in (c) and (d), respectively.

9. *CP* violation in $B^{-} \to \rho^{0}\pi^{-}$

As noticed in passing, *CP* asymmetry for the quasi-two-body decay $B^{-} \to \rho^{0}\pi^{-}$ was found by LHCb to be consistent with zero in all three *S*-wave approaches (cf. Table V).[9] Indeed, if this quasi-two-body *CP* asymmetry is nonzero, it will destroy the interference pattern observed in Fig. 2, see the first term in Eq. (3.23). However, the existing theoretical predictions based on QCD factorization (QCDF) [49,59], perturbative QCD (pQCD) [60], soft-collinear effective theory (SCET) [61], topological diagram approach (TDA) [62] and factorization-assisted topological-amplitude (FAT) approach [63] all lead to a negative *CP* asymmetry for $B^{-} \to \rho^{0}\pi^{-}$, ranging from -7% to -45% (see Table VIII).

It has been argued in [64] that in $B \to PV$ decays with $m_{V} < 1$ GeV, for example, $V = \rho(770)$ or $K^{*}(892)$, *CP* asymmetry induced from a short-distance mechanism is suppressed by the *CPT* constraint. Under the $2 + 1$

approximation that the resonances produced in heavy meson decays do not interact with the third particle, there do not exist other states which can be connected to $\pi\pi$ or πK through final-state interactions. Hence, the absence of final-state interactions implies the impossibility to observe *CP* asymmetry in those processes. However, if we take this argument seriously to explain the approximately vanishing *CP* asymmetry in $B^{+} \to \rho^{0}\pi^{+}$, it will be at odd with the *CP* violation seen in other *PV* modeds. For example, *CP* violation in the decay $B^{0} \to K^{*+}\pi^{-}$ with $\mathcal{A}_{CP} = -0.308 \pm 0.062$ was clearly observed by the LHCb [65]. Therefore, it appears that the smallness of $\mathcal{A}_{CP}(B^{+} \to \rho^{0}\pi^{+})$ has nothing to do with the *CPT* constraint.

As elucidated in [66], the nearly vanishing *CP* violation in $B^{-} \to \rho^{0}\pi^{-}$ is understandable in the QCD factorization approach. There are two kinds of $1/m_{b}$ corrections in QCDF: penguin annihilation to the penguin amplitude and hard spectator interactions to the flavor operator a_{2}. Power corrections in QCDF often involve endpoint divergences which are parametrized in terms of the parameters ρ_{A}, ϕ_{A} for penguin annihilation and ρ_{H}, ϕ_{H} for hard spectator interactions (see Eq. (B4) in Appendix B). In the heavy

---

[9]There was a measurement of $\mathcal{A}_{CP}(\rho^{0}\pi^{-})$ by *BABAR* with the result $0.18 \pm 0.07^{+0.05}_{-0.15}$ from a Dalitz plot analysis of $B^{-} \to \pi^{+}\pi^{-}\pi^{-}$ [7].

TABLE VIII. Theoretical predictions of CP violation (in %) for the $B^- \to \rho^0 \pi^-$ decay in various approaches.

QCDF [49]	QCDF [59]	pQCD [60]	SCET [61]	TDA [62]	FAT [63]
$-9.8^{+3.4+11.4}_{-2.6-10.2}$	$-6.7^{+0.2+3.2}_{-0.2-3.7}$	$-27.5^{+2.3+0.9}_{-3.1-1.0} \pm 1.4 \pm 0.9$	$-19.2^{+15.5+1.7}_{-13.4-1.9}$	-23.9 ± 8.4	-45 ± 4

quark limit, $\mathcal{A}_{CP}(\rho^0 \pi^-)$ is of order 6.3%. Power corrections induced from hard spectator interactions will push it up further, say $\mathcal{A}_{CP}(\rho^0 \pi^-) \sim 15\%$, whereas penguin annihilation will pull it to the opposite direction (see Table III of [66]). Owing to the destructive contributions from these two different $1/m_b$ power corrections, a nearly vanishing $\mathcal{A}_{CP}(\rho^0 \pi^-)$ can be *accommodated* in QCDF. For example, $\mathcal{B}(\rho^0 \pi^-) \approx 8.4 \times 10^{-6}$ and $\mathcal{A}_{CP}(\rho^0 \pi^-) \approx (-0.7^{+5.4}_{-4.5})\%$ are obtained with $(\rho_H, \rho_A^i, \rho_A^f) = (3.15, 3.08, 0.83)$ and $(\phi_H, \phi_A^i, \phi_A^f) = (-113°, -145°, -36°)$ [66], while experimentally $\mathcal{B}(\rho^0 \pi^-) = (8.3^{+1.2}_{-1.3}) \times 10^{-6}$ [48] and $\mathcal{A}_{CP}(\rho^0 \pi^-) = (0.7 \pm 1.9)\%$ in the isobar model.

10. CP violation at high m_{high}

An inspection of Fig. 1 for CP asymmetries measured in the high invariant-masss region, the peak in the high-m_{high} region could be ascribed to the $\chi_{c0}(1P)$ resonance with a mass 3414.71 ± 0.30 MeV and a width 10.8 ± 0.6 MeV. As stressed in [67], although LHCb has not yet found the contribution from the $B^- \to \pi^- \chi_{c0}$ amplitude in $B^- \to \pi^+ \pi^- \pi^-$ decay, the Mirandizing distribution for Run I data has already shown a clear and huge CP asymmetry around the χ_{c0} invariant mass. We also see from Fig. 1 that CP asymmetry in the high-m_{high} region changes sign at around 4 GeV, near the $D\bar{D}$ threshold. In analog to the $\pi\pi \leftrightarrow K\bar{K}$ rescattering in the low mass region, final-state rescattering $D\bar{D} \to P\bar{P}$ could provide the strong phases necessary for CP violation in the high-m_{high} region [67,68]. However, we will not address this issue in this work.

IV. CONCLUSIONS

We have presented in this work a study of charmless three-body decays of B mesons $B^- \to K^+ K^- \pi^-$ and $B^- \to \pi^+ \pi^- \pi^-$ based on the factorization approach. Our main results are:

(i) There are two distinct sources of nonresonant contributions: one arises from the $b \to u$ tree transition and the other from the nonresonant matrix element of scalar densities $\langle M_1 M_2 | \bar{q}_1 q_2 | 0 \rangle^{NR}$. It turns out that even for tree-dominated three-body decays $B \to \pi\pi\pi$ and $K\bar{K}\pi$, nonresonant contributions are dominated by the penguin mechanism rather than by the $b \to u$ tree process, as implied by the large nonresonant component observed in the $\pi^- K^+$ system which accounts for one third of the $B^- \to K^+ K^- \pi^-$ rate. We have identified the nonresonant contribution to the $\pi^- K^+$ system with the matrix element $\langle \pi^- K^+ | \bar{d}s | 0 \rangle^{NR}$.

(ii) The calculated branching fraction of $B^- \to f_2(1270)\pi^- \to K^+ K^- \pi^-$ is smaller than experiment by a factor of ~ 7 in its central value. Nevertheless, the same form factor for $B \to f_2(1270)$ transition leads to a prediction of $\mathcal{B}(B^- \to f_2(1270)\pi^- \to \pi^+ \pi^- \pi^-)$ in agreement with the experimental value. Branching fractions of $B^- \to f_2(1270)\pi^-$ extracted from the measured rates of $B^- \to f_2(1270)\pi^- \to K^+ K^- \pi^-$ and $B^- \to f_2(1270)\pi^- \to \pi^+ \pi^- \pi^-$ by the LHCb also differ by a factor of seven. This together with the theoretical predictions of $\mathcal{B}(B^- \to f_2(1270)\pi^-)$ leads us to conjecture that the $f_2(1270)$ contribution to $B^- \to K^+ K^- \pi^-$ is largely overestimated experimentally. This needs to be clarified in the Run II experiment. Including $1/m_b$ power corrections from penguin annihilation inferred from QCDF, a sizable CP asymmetry of 32% in the $f_2(1270)$ component are in accordance with the LHCb measurement.

(iii) A fraction of 5% for the $\rho(1450)$ component in $B^- \to \pi^+ \pi^- \pi^-$ is in accordance with the theoretical expectation. However, a large fraction of 30% in $B^- \to K^+ K^- \pi^-$ is entirely unexpected. If this feature is confirmed in the future, it is likely that the broad vector resonance $\rho(1450)$ may play the role of the s-called $f_X(1500)$ broad resonance observed in $B \to KKK$ and $K\bar{K}\pi$ decays.

(iv) The contribution of $K_0^*(1430)^0$ to $B^- \to K^+ K^- \pi^-$ was found to be too large by a factor of 3 when confronted with experiment. The current theoretical predictions based on both QCDF and pQCD for $\mathcal{B}(B^- \to K_0^*(1430)^0 K^-)$ are also too large compared to experiment. This issue needs to be resolved.

(v) By varying the relative phase between A_σ and $A_{NR}^{\pi^+\pi^+}$, we find that a large and negative CP asymmetry of -66% through the S-wave $\pi^+ \pi^- \to K^+ K^-$ rescattering can be accommodated at $\phi_\sigma \approx 134°$. However, the predicted branching fraction is less than the LHCb value by a factor of 4! This is ascribed to the fact that one should use Eq. (2.25) to describe $\pi\pi \leftrightarrow K\bar{K}$ final-state rescattering. By the same token, the branching fraction of the rescattering contribution to $B^- \to \pi^+ \pi^- \pi^-$ also seems to be overestimated experimentally by a factor of 4.

(vi) Using the QCDF expression of the $B^- \to \sigma\pi^-$ amplitude to compute $B^- \to \sigma\pi^- \to \pi^+ \pi^- \pi^-$, the resultant CP violation of 15% and branching fraction agree with experiment.

(vii) *CP* asymmetry for the dominant quasi-two-body decay mode $B^- \to \rho^0 \pi^-$ was found by the LHCb to be consistent with zero in all three *S*-wave models. In the QCD factorization approach, the $1/m_b$ power corrections, namely penguin annihilation and hard spectator interactions, contribute destructively to $\mathcal{A}_{CP}(B^- \to \rho^0 \pi^-)$ to render it consistent with zero.

(viii) While *CP* violation in $B^- \to \rho^0 \pi^-$ is consistent with zero, a significant *CP* asymmetry has been seen in the $\rho^0(770)$ region where the data are separated by the sign of the value of $\cos\theta$ with θ being the angle between the pions with the same-sign charge. Considering the low $\pi^+ \pi^-$ invariant mass region of the $B^+ \to \pi^+ \pi^+ \pi^-$ Dalitz plot of *CP* asymmetries divided into four zones as depicted in Fig. 4, we have predicated the sign of *CP* violation in each zone correctly which arises from the interference between the $\rho(770)$ and σ as well as the nonresonant background.

ACKNOWLEDGMENTS

APPENDIX A: INPUT PARAMETERS

Many of the input parameters for the decay constants of pseudoscalar and vector mesons and form factors for $B \to P, V$ transitions can be found in [49] where uncertainties in form factors are shown. The reader is referred to [53] for decay constants and form factors related to scalar mesons. For reader's convenience, we list the scalar decay constants relevant to this work

$$\bar{f}_{f_0} = 460, \qquad \bar{f}_\sigma^u = 350, \qquad \bar{f}_{K_0^*(1430)} = 550, \quad \text{(A1)}$$

defined at $\mu = 1$ GeV and expressed in units of MeV. The vector decay constant of $K_0^*(1430)$ is related to the scalar one via

$$f_{K_0^*} = \frac{m_s(\mu) - m_q(\mu)}{m_{K_0^*}} \bar{f}_{K_0^*}. \qquad \text{(A2)}$$

The form factors used in this work are

$$F_0^{B\pi}(0) = 0.25 \pm 0.03, \qquad F_0^{BK}(0) = 0.35 \pm 0.04,$$
$$A_0^{B\rho}(0) = 0.303 \pm 0.029, \qquad A_0^{B\omega}(0) = 0.281 \pm 0.030,$$
$$A_0^{Bf_2}(0) = 0.13 \pm 0.02, \qquad F^{B\sigma^u}(0) = 0.25 \pm 0.02,$$
$$A_2^{B\rho}(0) = 0.221 \pm 0.023, \qquad A_2^{B\omega}(0) = 0.198 \pm 0.023. \qquad \text{(A3)}$$

The $B \to f_2(1270)$ transition form factor taken from [19] is evaluated using large energy effective theory, while the form factors for $B \to V$ transition are from [69]. There is an updated light-cone sum-rule analysis of $B \to V$ transition form factors in [70] in which one has

$$A_0^{B\rho}(0) = 0.356 \pm 0.042, \qquad A_0^{B\omega}(0) = 0.328 \pm 0.048. \qquad \text{(A4)}$$

However, we will not use this new analysis in this study for two reasons. First, it will lead to too large $B^- \to \rho^0 \pi^-$ and $B^- \to \omega \pi^-$ rates compared to experiment. Second, the parameters (ρ_A, ϕ_A) and (ρ_H, ϕ_H), which govern $1/m_b$ power corrections from penguin annihilation and hard spectator interactions, respectively, have been extracted from the data using $B \to V$ from factors given by [69], see Appendix B below.

Note that for the σ meson, the Clebsch-Gordon coefficient $1/\sqrt{2}$ is already included in $\bar{f}_\sigma^u$ and $F_0^{B\sigma^u}$. For the $f_0(980)$, one needs to multiple a factor of $\sin\theta/\sqrt{2}$ to get its decay constant and form factor, for example, $\bar{f}_{f_0(980)}^u = \bar{f}_{f_0(980)} \sin\theta/\sqrt{2}$ with the mixing angle $\theta \approx 20°$.

For the Cabibbo-Kobayashi-Maskawa (CKM) matrix elements, we use the updated Wolfenstein parameters $A = 0.8235$, $\lambda = 0.224837$, $\bar{\rho} = 0.1569$ and $\bar{\eta} = 0.3499$ [71]. The corresponding CKM angles are $\sin 2\beta = 0.7083^{+0.0127}_{-0.0098}$ and $\gamma = (65.80^{+0.94}_{-1.29})°$ [71].

Among the quarks, the strange quark gives the major theoretical uncertainty to the decay amplitude. Hence, we will only consider the uncertainty in the strange quark mass given by $m_s(2 \text{ GeV}) = 92.0 \pm 1.1$ MeV [72].

APPENDIX B: FLAVOR OPERATORS

In our previous works [8–10], we have employed the values of the flavor operators a_i^p given in [8] at the renormalization scale $\mu = \bar{m}_b/2 = 2.1$ GeV. Since then, there is a substantial progress in the determination of $1/m_b$ power corrections to a_i^p. In the QCD factorization approach, flavor operators have the expressions [20,73]

$$a_i^p(M_1 M_2) = \left(c_i + \frac{c_{i\pm1}}{N_c} \right) N_i(M_2) + \frac{c_{i\pm1}}{N_c} \frac{C_F \alpha_s}{4\pi}$$
$$\times \left[V_i(M_2) + \frac{4\pi^2}{N_c} H_i(M_1 M_2) \right] + P_i^p(M_2), \qquad \text{(B1)}$$

where $i = 1, …, 10$, the upper (lower) signs apply when i is odd (even), c_i are the Wilson coefficients, $C_F = (N_c^2 - 1)/(2N_c)$ with $N_c = 3$, M_2 is the emitted meson and M_1 shares the same spectator quark with the B meson. The quantities $V_i(M_2)$ account for vertex corrections, $H_i(M_1 M_2)$ for hard spectator interactions with a hard

gluon exchange between the emitted meson and the spectator quark of the B meson and $P_i^p(M_2)$ for penguin contractions.

In the QCD factorization approach, there are two kinds of $1/m_b$ corrections: penguin annihilation to the penguin amplitude and hard spectator interactions to a_2:

$$P = P_{\text{SD}} + 1/m_b \text{corrections}$$

$$\propto [\lambda_u(a_4^u + r_\chi^P a_6^u) + \lambda_c(a_4^c + r_\chi^P a_6^c)] + \underbrace{\lambda_u \beta_3^u + \lambda_c \beta_3^c}_{\text{penguin annihilation}},$$

(B2)

and

$$a_2(M_1 M_2) = c_2 + \frac{c_1}{N_c} + \frac{c_1}{N_c} \frac{C_F \alpha_s}{4\pi}$$

$$\times \left[V_2(M_2) + \frac{4\pi^2}{N_c} H_2(M_1 M_2) \right]. \quad \text{(B3)}$$

Power corrections in QCDF often involve endpoint divergences. We shall follow [20] to model the endpoint divergence $X \equiv \int_0^1 dx/(1-x)$ in the penguin annihilation and hard spectator scattering diagrams as

$$X_A^{i,f} = \ln\left(\frac{m_B}{\Lambda_h}\right)(1 + \rho_A^{i,f} e^{i\phi_A^{i,f}}),$$

$$X_H = \ln\left(\frac{m_B}{\Lambda_h}\right)(1 + \rho_H e^{i\phi_H}), \quad \text{(B4)}$$

with Λ_h being a typical hadronic scale of 0.5 GeV, where the superscripts "i" and "f" refer to gluon emission from the initial and final-state quarks, respectively. A fit of the four parameters $(\rho_A^{i,f}, \phi_A^{i,f})$ with the first order approximation of $\rho_H \approx \rho_A^i$ and $\phi_H \approx \phi_A^i$ to the $B \to PP$ and PV data yields [59,74]

$$(\rho_A^i, \rho_A^f)_{PP} = (2.98_{-0.86}^{+1.12}, 1.18_{-0.23}^{+0.20}),$$

$$(\phi_A^i, \phi_A^f)_{PP} = (-105_{-24}^{+34}, -40_{-8}^{+11})°, \quad \text{(B5)}$$

and

$$(\rho_A^i, \rho_A^f)_{PV} = (2.87_{-1.95}^{+0.66}, 0.91_{-0.13}^{+0.12}),$$

$$(\phi_A^i, \phi_A^f)_{PV} = (-145_{-21}^{+14}, -37_{-9}^{+10})°. \quad \text{(B6)}$$

In general, the difference between $a_i^p(M_2 M_1)$ and $a_i^p(M_1 M_2)$ is small for the quasi-two-body decays $B \to PV$ except for $a_{6,8}^p$. Using Eq. (B6) as an input for $1/m_b$ power corrections and taking the averages of $a_i^p(PV)$ and $a_i^p(VP)$ (except for $a_{6,8}^p$), we have

$$a_1 \approx 0.988 \pm 0.102i, \qquad a_2 \approx 0.183 - 0.348i, \qquad a_3 \approx -0.0023 + 0.0174i, \qquad a_5 \approx 0.00644 - 0.0231i,$$

$$a_4^u \approx -0.025 - 0.021i, \qquad a_4^c \approx -0.030 - 0.012i, \qquad a_6^u \approx -0.042 - 0.014i, \qquad a_6^c \approx -0.045 - 0.005i,$$

$$a_7 \approx (-0.5 + 2.7i) \times 10^{-4}, \qquad a_8^u \approx (5.2 - 1.0i) \times 10^{-4}, \qquad a_8^c \approx (5.0 - 0.5i) \times 10^{-4},$$

$$a_9 \approx (-8.9 - 0.9i) \times 10^{-3}, \qquad a_{10}^u \approx (-1.45 + 3.12i) \times 10^{-3}, \qquad a_{10}^c \approx (-1.51 + 3.17i) \times 10^{-3}, \quad \text{(B7)}$$

at the renormalization scale $\mu = \bar{m}_b(\bar{m}_b) = 4.18$ GeV, where the values of $a_{6,8}^p$ are for $M_1 M_2 = VP$. For $M_1 M_2 = PV$ we should use

$$a_6^u(PV) \approx -0.010 - 0.015i, \qquad a_6^c(PV) \approx -0.013 - 0.006i,$$

$$a_8^u(PV) \approx -(8.9 + 8.5i) \times 10^{-5}, \qquad a_8^c(PV) \approx -(10.7 + 3.7i) \times 10^{-4}. \quad \text{(B8)}$$

There are two different sources for the strong phases of a_i^p: (i) vertex corrections, hard spectator interactions and penguin contractions which are perturbatively calculable in the QCD factorization approach [20] and (ii) $1/m_b$ power corrections.

Note that the parameter $N_i(M)$ in Eq. (B1) vanishes if M is a tensor meson or a vector meson with $i = 6, 8$, or a neutral scalar meson such as σ, f_0 and a_0^0 with $i \neq 6, 8$. Otherwise, it is equal to one. Consequently, the flavor

operators given in Eqs. (B7) and (B8) are not applicable to the quasi-two-body decays $B \to SP$ ($S = \sigma$ or f_0) for two reasons. First, $N_i(\sigma) = 0$ means that $a_i^p(P\sigma)$ do not receive factorizable contributions except for $i = 6, 8$. Second, light-cone distribution amplitudes (LCDAs) of scalar and pseudoscalar mesons have different behavior. While the symmetric pion LCDA peaks at $x = 1/2$, the antisymmetric LCDA of the light scalar such as σ peaks at $x = 0.25$ and 0.75. As a result, $a_i^p(\sigma P)$ and $a_i^p(P\sigma)$ can be quite

TABLE IX. Numerical values of the flavor operators $a_i^p(M_1M_2)$ for $M_1M_2 = \sigma\pi$ and $\pi\sigma$ at the scale $\mu = \bar{m}_b(\bar{m}_b) = 4.18$ GeV [66]. In this work we use the same set of flavor operators to work out $B \to f_0(980)\pi$ decays.

a_i^p	$\sigma\pi$	$\pi\sigma$	a_i^p	$\sigma\pi$	$\pi\sigma$
a_1	$0.95 + 0.014i$	$0.015 - 0.004i$	a_6^c	$-0.045 - 0.005i$	$-0.045 - 0.005i$
a_2	$0.33 - 0.080i$	$-0.056 + 0.024i$	a_7	$(-1.8 + 0.3i)10^{-4}$	$(-4.2 + 1.0i)10^{-5}$
a_3	$-0.009 + 0.003i$	$0.0026 - 0.0008i$	a_8^u	$(4.8 - 1.0i)10^{-4}$	$(4.8 - 1.0i)10^{-4}$
a_4^u	$-0.022 - 0.015i$	$0.062 - 0.013i$	a_8^c	$(4.6 - 0.5i)10^{-4}$	$(4.6 - 0.5i)10^{-4}$
a_4^c	$-0.027 - 0.006i$	$-0.012 - 0.007i$	a_9	$(-8.6 - 0.1i)10^{-3}$	$(-1.3 + 0.4i)10^{-4}$
a_5	$0.0158 - 0.003i$	$0.0035 - 0.0009i$	a_{10}^u	$(-2.6 + 0.6i)10^{-3}$	$(8.7 - 3.1i)10^{-4}$
a_6^u	$-0.042 - 0.014i$	$-0.042 - 0.014i$	a_{10}^c	$(-2.6 + 0.7i)10^{-3}$	$(4.6 - 2.8i)10^{-4}$

different except for $a_{6,8}^p$. As an example, numerical values of the flavor operators $a_i^p(M_1M_2)$ for $M_1M_2 = \sigma\pi$ and $\pi\sigma$ are shown in Table IX. We see that, for instance, $a_1(\pi\sigma) = 0.015 - 0.004i$ is very different from $a_1(\sigma\pi) = 0.95 + 0.014i$. In practice, we also use the same set of flavor operators to work out $B \to f_0(980)\pi$ decays.

APPENDIX C: FINAL STATE INTERACTIONS

Since there is some confusion in the literature concerning the rescattering formula, we believe that it will be useful to go through the relevant derivations. Our discussion follows Refs. [35,37] closely. The weak Hamiltonian is given by $H_W = \sum_q \lambda_q O_q$, where λ_q are $V_{qb}V_{qd}^*$ and O_q are four-quark operators with Wilson coefficients included. From the time reversal invariance of O_q, it follows that

$$(\langle i; \text{out}|O_q|\bar{B}\rangle)^* = (\langle i; \text{out}|)^* U_T^\dagger U_T O_q^* U_T^\dagger U_T|\bar{B}\rangle^*$$
$$= \langle i; \text{in}|O_q|\bar{B}\rangle, \qquad (C1)$$

which can be expressed as

$$(\langle i; \text{out}|O_q|\bar{B}\rangle)^* = \sum_k \langle i; \text{in}|k; \text{out}\rangle\langle k; \text{out}|O_q|\bar{B}\rangle$$
$$= \sum_k \mathcal{S}_{ik}^\dagger \langle k; \text{out}|O_q|\bar{B}\rangle, \qquad (C2)$$

where $\mathcal{S}_{ik} \equiv \langle i; \text{out}|k; \text{in}\rangle$ denotes the strong interaction S-matrix element. Note that we have used $U_T(|\text{out}(\text{in})\rangle)^* = |\text{in}(\text{out})\rangle$ to fix the phase convention, which also leads to

$$\mathcal{S}_{ij}^* = (\langle i; \text{out}|)^* U_T^\dagger U_T(|j; \text{in}\rangle)^* = \langle i; \text{in}|j; \text{out}\rangle = \mathcal{S}_{ji}^*. \qquad (C3)$$

From the following identity

$$\sum_k \mathcal{S}_{ik}^\dagger \mathcal{S}_{kj}^{1/2} = (\mathcal{S}^{1/2})_{ij}^\dagger = (\mathcal{S}^{1/2})_{ji}^* = (\mathcal{S}^{1/2})_{ij}^*, \qquad (C4)$$

where use of Eq. (C3) has been made, it is clear that the solution of Eq. (C2) is simply [36]

$$\langle i; \text{out}|O_q|\bar{B}\rangle = \sum_j \mathcal{S}_{ij}^{1/2} \mathcal{A}_{0j}^q, \qquad (C5)$$

where $\mathcal{A}_{0j}^q$ is a real amplitude. The weak decay amplitude picks up strong scattering phases [75] and finally we have [35]

$$\langle i; \text{out}|H_W|\bar{B}\rangle = \sum_q \langle i; \text{out}|\lambda_q O_q|\bar{B}\rangle$$
$$= \sum_{q,j} \mathcal{S}_{ij}^{1/2}(\lambda_q \mathcal{A}_{0j}^q) = \sum_j \mathcal{S}_{ij}^{1/2} \mathcal{A}_{0j}, \qquad (C6)$$

where we have defined $\mathcal{A}_0 \equiv \sum_q \lambda_q \mathcal{A}_0^q$ and, consequently, it is free of any strong phase.

It will be useful to give an equivalent expression to the above results in terms of time evolution operator [37]. It is well known that the so-called "in" and "out" states can be expressed as

$$|i; \text{in}\rangle = \lim_{T\to\infty} U_I(0, -T)|i; \text{free}\rangle,$$
$$|i; \text{out}\rangle = \lim_{T\to\infty} U_I(0, T)|i; \text{free}\rangle, \qquad (C7)$$

with $U_I(t_2, t_1)$ the time evolution operator in the interaction picture given by

$$U_I(t_2, t_1) = e^{iH_0 t_2} e^{-iH(t_2 - t_1)} e^{-iH_0 t_1}$$
$$= e^{iH_0 t_2} U(t_2, t_1) e^{-iH_0 t_1}, \qquad (C8)$$

where H_0 is the free Hamiltonian and H is the full strong Hamiltonian. The time evolution operator satisfies $U_T^\dagger U_I^*(t_2, t_1) U_T = U_I(-t_2, -t_1)$ and $U_I^\dagger(t_2, t_1) = U_I(t_1, t_2)$, as H_0 and H are time-invariant and Hermitian.

The amplitude $\langle i; \text{out}|O_q|\bar{B}\rangle$ can now be expressed as

$$\langle i; \text{out}|O_q|\bar{B}\rangle = \lim_{T\to\infty} \langle i; \text{free}|U_I(T, 0)O_q|\bar{B}\rangle, \qquad (C9)$$

and the previous derivations can all be brought through parallelly with the help of $U_T(|i; \text{free}\rangle)^* = |i; \text{free}\rangle$ matching the phase convention and the time invariant properties of H_0 and H. Indeed, from

$$U_T^\dagger U_I^*(T,0)U_T = U_I(-T,0) = U_I(-T,T)U_I(T,0)$$
$$= U_I^\dagger(T,-T)U(T,0), \qquad \text{(C10)}$$

and

$$\mathcal{S}_{ij} \equiv \langle i; \text{out}|j; \text{in}\rangle = \lim_{T\to\infty} \langle i; \text{free}|U_I(T,-T)|j; \text{free}\rangle, \quad \text{(C11)}$$

we have

$$\left(\lim_{T\to\infty} \langle i; \text{free}|U_I(T,0)O_q|\bar{B}\rangle \right)^*$$
$$= \sum_k \lim_{T\to\infty} \langle i; \text{free}|U_I^\dagger(T,-T)|k, \text{free}\rangle$$
$$\times \langle k; \text{free}|U_I(T,0)O_q|\bar{B}\rangle, \qquad \text{(C12)}$$

which is equivalent to Eq. (C2). Furthermore, using Eq. (C8) and the fact that $|i, \text{free}\rangle$ and $|j, \text{free}\rangle$ are degenerate eigenstates of H_0, we are led to

$$\langle i; \text{free}|U_I(T,0)|j; \text{free}\rangle = \langle i; \text{free}|U_I(0,-T)|j; \text{free}\rangle$$
$$= \langle i; \text{free}|U_I(T/2,-T/2)|j; \text{free}\rangle, \qquad \text{(C13)}$$

which justifies the following definition,

$$\mathcal{S}_{ij}^{1/2} \equiv \lim_{T\to\infty} \langle i; \text{free}|U_I(T,0)|j; \text{free}\rangle, \qquad \text{(C14)}$$

and, consequently, with $\mathcal{A}_{0j}^q \equiv \langle j; \text{free}|O_q|\bar{B}\rangle$, we obtain

$$\langle i; \text{out}|Q_q|\bar{B}\rangle = \lim_{T\to\infty} \langle i; \text{free}|U_I(T,0)O_q|\bar{B}\rangle$$
$$= \sum_j \mathcal{S}_{ij}^{1/2} \langle j; \text{free}|O_q|\bar{B}\rangle$$
$$= \sum_j \mathcal{S}_{ij}^{1/2} \mathcal{A}_{0j}^q, \qquad \text{(C15)}$$

which corresponds to Eq. (C5), and Eq. (C6) follows accordingly. Note that $\mathcal{A}_{0j}^q = (\mathcal{A}_{0j}^q)^*$ is a consequence of the phase convention and the time invariant property of O_q.

It is useful to express Eq. (C6) in terms of the full time-evolution operator,

$$\langle i; \text{out}|H_W|\bar{B}\rangle = \lim_{T\to\infty} \langle i; \text{free}|e^{iH_0 T}U(T,0)H_W|\bar{B}\rangle, \quad \text{(C16)}$$

which can be decomposed into (with $\tau \gtrsim 0$)

$$\langle i; \text{out}|H_W|\bar{B}\rangle = \sum_j \lim_{T\to\infty} \langle i; \text{free}|e^{iH_0 T}U(T,\tau)e^{-iH_0\tau}|j, \text{free}\rangle$$
$$\times \langle j; \text{free}|e^{iH_0\tau}U(\tau,0)H_W|\bar{B}\rangle. \qquad \text{(C17)}$$

The above expression clearly shows the time evolution nature of rescattering [38] and the rescattering of $\pi\pi \to K\bar{K}$ is considered to happen at a much later stage of time-evolution contained in $\langle i; \text{free}|e^{iH_0 T}U(T,\tau)e^{-iH_0\tau}|j, \text{free}\rangle$, while all the violent and rapid interactions have already happened and are contained in $\langle j; \text{free}|e^{iH_0\tau}U(\tau,0)H_W|\bar{B}\rangle$.

---

[1] R. Aaij *et al.* (LHCb Collaboration), Measurement of *CP* Violation in the Phase Space of $B^\pm \to K^\pm\pi^+\pi^-$ and $B^\pm \to K^\pm K^+K^-$ Decays, Phys. Rev. Lett. **111**, 101801 (2013).

[2] R. Aaij *et al.* (LHCb Collaboration), Measurement of *CP* Violation in the Phase Space of $B^\pm \to K^+K^-\pi^\pm$ and $B^\pm \to \pi^+\pi^-\pi^\pm$ Decays, Phys. Rev. Lett. **112**, 011801 (2014).

[3] R. Aaij *et al.* (LHCb Collaboration), Measurements of *CP* violation in the three-body phase space of charmless $B^\pm$ decays, Phys. Rev. D **90**, 112004 (2014).

[4] R. Aaij *et al.* (LHCb Collaboration), Amplitude Analysis of $B^\pm \to \pi^\pm K^+K^-$ Decays, Phys. Rev. Lett. **123**, 231802 (2019).

[5] R. Aaij *et al.* (LHCb Collaboration), Observation of Several Sources of *CP* Violation in $B^+ \to \pi^+\pi^+\pi^-$ Decays, Phys. Rev. Lett. **124**, 031801 (2020).

[6] R. Aaij *et al.* (LHCb Collaboration), Amplitude analysis of the $B^+ \to \pi^+\pi^+\pi^-$ decay, Phys. Rev. D **101**, 012006 (2020).

[7] B. Aubert *et al.* (*BABAR* Collaboration), Dalitz plot analysis of $B^+ \to \pi^+\pi^+\pi^-$ decays, Phys. Rev. D **79**, 072006 (2009).

[8] H. Y. Cheng, C. K. Chua, and A. Soni, Charmless three-body decays of *B* mesons, Phys. Rev. D **76**, 094006 (2007).

[9] H. Y. Cheng and C. K. Chua, Branching fractions and direct *CP* violation in charmless three-body decays of *B* mesons, Phys. Rev. D **88**, 114014 (2013).

[10] H. Y. Cheng, C. K. Chua, and Z. Q. Zhang, Direct *CP* violation in charmless three-body decays of *B* mesons, Phys. Rev. D **94**, 094015 (2016).

[11] W. F. Wang, H. C. Hu, H. n. Li, and C. D. Lu, Direct *CP* asymmetries of three-body *B* decays in perturbative QCD, Phys. Rev. D **89**, 074031 (2014).

[12] S. Kräkl, T. Mannel, and J. Virto, Three-body non-leptonic B decays and QCD factorization, Nucl. Phys. **B899**, 247 (2015).

[13] R. Klein, T. Mannel, J. Virto, and K. K. Vos, *CP* violation in multibody *B* decays from QCD factorization, J. High Energy Phys. 10 (2017) 117.

[14] B. Aubert *et al.* (*BABAR* Collaboration), Observation of the Decay $B^+ \to K^+K^-\pi^+$, Phys. Rev. Lett. **99**, 221801 (2007).

[15] C.-L. Hsu *et al.* (Belle Collaboration), Measurement of branching fraction and direct *CP* asymmetry in charmless

$B^+ \to K^+ K^- \pi^+$ decays at Belle, Phys. Rev. D **96,** 031101 (2017).

[16] M. Wirbel, B. Stech, and M. Bauer, Exclusive semileptonic decays of heavy mesons, Z. Phys. C **29,** 637 (1985); M. Bauer, B. Stech, and M. Wirbel, Exclusive nonleptonic decays of D, D_s, and B mesons, Z. Phys. C **34,** 103 (1987).

[17] H. Y. Cheng, C. K. Chua, and C. W. Hwang, Covariant light front approach for s wave and p wave mesons: Its application to decay constants and form-factors, Phys. Rev. D **69,** 074025 (2004).

[18] W. Wang, B to tensor meson form factors in the perturbative QCD approach, Phys. Rev. D **83,** 014008 (2011).

[19] H. Y. Cheng and K. C. Yang, Charmless hadronic B decays into a tensor meson, Phys. Rev. D **83,** 034001 (2011).

[20] M. Beneke, G. Buchalla, M. Neubert, and C. T. Sachrajda, QCD Factorization for $B \to PP$ Decays: Strong Phases and *CP* Violation in the Heavy Quark Limit, Phys. Rev. Lett. **83,** 1914 (1999); QCD factorization for exclusive, nonleptonic B meson decays: General arguments and the case of heavy light final states, Nucl. Phys. **B591,** 313 (2000).

[21] J. P. Dedonder, A. Furman, R. Kaminski, L. Lesniak, and B. Loiseau, *S*-, *P*- and *D*-wave final state interactions and *CP* violation in $B^\pm \to \pi^\pm \pi^\mp \pi^\pm$ decays, Acta Phys. Pol. B **42,** 2013 (2011).

[22] C. L. Y. Lee, M. Lu, and M. B. Wise, $B_{\ell 4}$ and $D_{\ell 4}$ decays, Phys. Rev. D **46,** 5040 (1992).

[23] S. Fajfer, R. J. Oakes, and T. N. Pham, The penguin operators in nonresonant $B^- \to M \bar{M} \pi^- (M = \pi^-, K^-, K^0)$ decays, Phys. Rev. D **60,** 054029 (1999).

[24] S. Faller, T. Feldmann, A. Khodjamirian, T. Mannel, and D. van Dyk, Disentangling the decay observables in $B^- \to \pi^+ \pi^- \ell^- \bar{\nu}_\ell$, Phys. Rev. D **89,** 014015 (2014).

[25] X. W. Kang, B. Kubis, C. Hanhart, and U. G. Meißner, B_{l4} decays and the extraction of $|V_{ub}|$, Phys. Rev. D **89,** 053015 (2014).

[26] C. Hambrock and A. Khodjamirian, Form factors in $\bar{B}^0 \to \pi\pi\ell\bar{\nu}_\ell$ from QCD light-cone sum rules, Nucl. Phys. **B905,** 373 (2016).

[27] P. Böer, T. Feldmann, and D. van Dyk, QCD factorization theorem for $B \to \pi\pi\ell\nu$ decays at large dipion masses, J. High Energy Phys. 02 (2017) 133.

[28] S. Cheng, A. Khodjamirian, and J. Virto, $B \to \pi\pi$ form factors from light-cone sum rules with *B*-meson distribution amplitudes, J. High Energy Phys. 05 (2017) 157.

[29] S. Cheng, A. Khodjamirian, and J. Virto, Timelike-helicity $B \to \pi\pi$ form factor from light-cone sum rules with dipion distribution amplitudes, Phys. Rev. D **96,** 051901 (2017).

[30] S. Cheng, Dipion light-cone distribution amplitudes and $B \to \pi\pi$ form factors, Phys. Rev. D **99,** 053005 (2019).

[31] B. Aubert *et al.* (BABAR Collaboration), Measurements of *CP*-Violating Asymmetries in the Decay $B^0 \to K^+ K^- K^0$, Phys. Rev. Lett. **99,** 161802 (2007).

[32] G. W. S. Hou, Curious link of exclusive and inclusive CPV in charmless 3-body B^+ decays, arXiv:1911.06966.

[33] J. R. Pelaez and F. J. Yndurain, The pion-pion scattering amplitude, Phys. Rev. D **71,** 074016 (2005).

[34] J. H. Alvarenga Nogueira, I. Bediaga, A. B. R. Cavalcante, T. Frederico, and O. Lourenmo, *CP* violation: Dalitz interference, *CPT*, and final state interactions, Phys. Rev. D **92,** 054010 (2015).

[35] C. K. Chua, Rescattering effects in charmless $\bar{B}_{u,d,s} \to PP$ decays, Phys. Rev. D **78,** 076002 (2008).

[36] M. Suzuki and L. Wolfenstein, Final state interaction phase in B decays, Phys. Rev. D **60,** 074019 (1999).

[37] See Eq. (13.104) and the following discussion of T. D. Lee, Particle physics and introduction to field theory, Contemp. Concepts Phys. **1,** 1 (1981).

[38] W. S. Hou (private communication).

[39] I. Bediaga, T. Frederico, and O. Lourenco, *CP* violation and *CPT* invariance in $B^\pm$ decays with final state interactions, Phys. Rev. D **89,** 094013 (2014).

[40] F. Giacosa, T. Gutsche, V. Lyubovitskij, and A. Faessler, Decays of tensor mesons and the tensor glueball in an effective field approach, Phys. Rev. D **72,** 114021 (2005).

[41] M. Suzuki, Tensor meson dominance: Phenomenology of the f_2 meson, Phys. Rev. D **47,** 1043 (1993).

[42] H. M. Pilkuhn, *Relativistic Particle Physics* (Springer-Verlag, New York, 1979); see Tables 4–9.

[43] K. Abe *et al.* (Belle Collaboration), High statistics study of $f_0(980)$ resonance in $\gamma\gamma \to \pi^+\pi^-$ production, Phys. Rev. D **75,** 051101 (2007).

[44] J. P. Lees *et al.* (BABAR Collaboration), Dalitz plot analyses of $J/\psi \to \pi^+\pi^-\pi^0$, $J/\psi \to K^+K^-\pi^0$, and $J/\psi \to K_S^0 K^\pm \pi^\mp$ produced via e^+e^- annihilation with initial-state radiation, Phys. Rev. D **95,** 072007 (2017).

[45] W. F. Wang, Will the subprocesses $\rho(770, 1450)^0 \to K^+K^-$ contribute large branching fractions for $B^\pm \to \pi^\pm K^+K^-$ decays?, Phys. Rev. D **101,** 111901 (2020).

[46] J. P. Lees *et al.* (BABAR Collaboration), Study of *CP* violation in Dalitz-plot analyses of $B^0 \to K^+K^-K_S^0$, $B^+ \to K^+K^-K^+$, and $B^+ \to K_S^0 K_S^0 K^+$, Phys. Rev. D **85,** 112010 (2012).

[47] P. A. Zyla *et al.* (Particle Data Group), Review of particle physics, Prog. Theor. Exp. Phys. **2020,** 083C01 (2020).

[48] Y. Amhis *et al.* (HFLAV Collaboration), Averages of *b*-hadron, *c*-hadron, and τ-lepton properties as of summer 2016, Eur. Phys. J. C **77,** 895 (2017) and online update at https://hflav.web.cern.ch.

[49] H. Y. Cheng and C. K. Chua, Revisiting charmless hadronic $B_{u,d}$ decays in QCD factorization, Phys. Rev. D **80,** 114008 (2009).

[50] Y. Y. Fan and W. F. Wang, Resonance contributions $\phi(1020, 1680) \to K\bar{K}$ for the three-body decays $B \to K\bar{K}h$, Eur. Phys. J C **80,** 815 (2020).

[51] X. Liu and Z. J. Xiao, $B \to K_0^*(1430)K$ decays in perturbative QCD approach, Commun. Theor. Phys. **53,** 540 (2010).

[52] Y. Li, H. Y. Zhang, Y. Xing, Z. H. Li, and C. D. Lu, Study of $B \to K_0^*(1430)K^{(*)}$ decays in QCD factorization approach, Phys. Rev. D **91,** 074022 (2015).

[53] H. Y. Cheng, C. K. Chua, K. C. Yang, and Z. Q. Zhang, Revisiting charmless hadronic B decays to scalar mesons, Phys. Rev. D **87,** 114001 (2013).

[54] H. Y. Cheng, C. K. Chua, and K. C. Yang, Charmless hadronic B decays involving scalar mesons: Implications to the nature of light scalar mesons, Phys. Rev. D **73,** 014017 (2006).

[55] Y. Li, A. J. Ma, W. F. Wang, and Z. J. Xiao, Quasi-two-body decays $B_{(s)} \to P\rho'(1450), P\rho''(1700) \to P\pi\pi$ in the perturbative QCD approach, Phys. Rev. D **96,** 036014 (2017).

[56] J. J. Qi, Z. Y. Wang, X. H. Guo, and Z. H. Zhang, Study of localized *CP* violation in $B^- \to \pi^- \pi^+ \pi^-$ and the branching ratio of $B^- \to \sigma(600)\pi^-$ in the QCD factorization approach, Nucl. Phys. **B948**, 114788 (2019).

[57] C. Wang, Z. Y. Wang, Z. H. Zhang, and X. H. Guo, Localized direct *CP* violation for $B^\pm \to \rho^0(\omega)\pi^\pm \to \pi^+\pi^-\pi^\pm$ in QCD factorization, Phys. Rev. D **93**, 116008 (2016).

[58] A. C. dos Reis, *CP* violation in charmless $B^\pm$ three-body decays: where Flavour Physics meets Hadron Physics, J. Phys. Conf. Ser. **706**, 042001 (2016).

[59] J. Sun, Q. Chang, X. Hu, and Y. Yang, Constraints on hard spectator scattering and annihilation corrections in $B_{u,d} \to PV$ decays within QCD factorization, Phys. Lett. B **743**, 444 (2015).

[60] Y. Li, A. Ma, W. Wang, and Z. Xiao, Quasi-two-body decays $B_{(s)} \to P\rho \to P\pi\pi$ in perturbative QCD approach, Phys. Rev. D **95**, 056008 (2017).

[61] W. Wang, Y. M. Wang, D. S. Yang, and C. D. Lu, Charmless two-body $B_{(s)} \to VP$ decays in soft-collinear-effective-theory, Phys. Rev. D **78**, 034011 (2008).

[62] H. Y. Cheng, C. W. Chiang, and A. Kuo, Updating $B \to PP, VP$ decays in the framework of flavor symmetry, Phys. Rev. D **91**, 014011 (2015).

[63] S. Zhou, Q. Zhang, W. Lyu, and C. D. Lu, Analysis of charmless two-body B decays in factorization assisted topological amplitude approach, Eur. Phys. J. C **77**, 125 (2017).

[64] J. H. A. Nogueira, I. Bediaga, T. Frederico, P. C. Magalhaes, and J. M. Rodriguez, Suppressed $B \to PV$ *CP* asymmetry: *CPT* constraint, Phys. Rev. D **94**, 054028 (2016).

[65] R. Aaij *et al.* (LHCb Collaboration), Amplitude Analysis of the Decay $\bar{B}^0 \to K^0_S \pi^+ \pi^-$ and First Observation of the *CP* Asymmetry in $\bar{B}^0 \to K^*(892)^-\pi^+$, Phys. Rev. Lett. **120**, 261801 (2018).

[66] H. Y. Cheng, CP violation in $B^\pm \to \rho^0 \pi^\pm$ and $B^\pm \to \sigma\pi^\pm$ decays, arXiv:2005.06080.

[67] I. Bediaga, T. Frederico, and P. Magalhaes, *CP* asymmetry from hadronic charm rescattering in $B^\pm \to \pi^-\pi^+\pi^\pm$ decays at the high mass region, Phys. Lett. B **806**, 135490 (2020).

[68] T. Mannel, K. Olschewsky, and K. K. Vos, *CP* violation in three-body B decays: A model ansatz, J. High Energy Phys. 06 (2020) 073.

[69] P. Ball and R. Zwicky, $B_{d,s} \to \rho, \omega, K^*, \phi$ decay form-factors from light-cone sum rules revisited, Phys. Rev. D **71**, 014029 (2005).

[70] A. Bharucha, D. M. Straub, and R. Zwicky, $B \to V\ell^+\ell^-$ in the Standard Model from light-cone sum rules, J. High Energy Phys. 08 (2016) 098.

[71] J. Charles, A. Höcker, H. Lacker, S. Laplace, F. R. Le Diberder, J. Malclés, J. Ocariz, M. Pivk, and L. Roos (CKMfitter Group), *CP* violation and the CKM matrix: assessing the impact of the asymmetric *B* factories, Eur. Phys. J. C **41**, 1 (2005), updated results and plots available at: http://ckmfitter.in2p3.fr; M. Bona *et al.* (UTfit Collaboration), The 2004 UTfit collaboration report on the status of the unitarity triangle in the standard model, J. High Energy Phys. 07 (2005) 028; and updated results from http://utfit.roma1.infn.it.

[72] S. Aoki *et al.* (Flavour Lattice Averaging Group), FLAG Review 2019: Flavour Lattice Averaging Group (FLAG), Eur. Phys. J. C **80**, 113 (2020).

[73] M. Beneke and M. Neubert, QCD factorization for $B \to PP$ and $B \to PV$ decays, Nucl. Phys. **B675**, 333 (2003).

[74] Q. Chang, J. Sun, Y. Yang, and X. Li, A combined fit on the annihilation corrections in $B_{u,d,s} \to PP$ decays within QCDF, Phys. Lett. B **740**, 56 (2015).

[75] K. M. Watson, The effect of final state interactions on reaction cross-sections, Phys. Rev. **88**, 1163 (1952).